

ISOLDE NEWSLETTER 2019



New setups successfully used at ISOLDE in 2018: the SPEDE detector at IDS; the four HIE ISOLDE cryomodules; the ISS spectrometer and the WISARD inner detector.

- [Introduction](#)
- [Information for users coming to ISOLDE in 2019](#)

ISOLDE facility • [Target and Ion Source Development during LS2](#) • [RILIS operation and development: recent accomplishments and future plans](#) • [Dielectronic recombination at REXEBIS](#) • [Investigations for a future \$^{11}\text{C}\$ treatment facility Part 1: Production](#) • [Investigations for a future \$^{11}\text{C}\$ treatment facility Part 2: Charge breeding](#) • [Challenges in using a pepperpot emittance meter](#) • [MEDeGUN - a high-compression electron gun for an EBIS charge breeder](#)

Ground-state properties • [2018 at the Collinear Resonance Ionisation Spectroscopy \(CRIS\) experiment](#) • [Determination of the electron affinity of astatine](#) • [Laser spectroscopy on Ge isotopes across the \$N=40\$ subshell closure](#) • [Mass measurements of neutron-deficient indium isotopes at the extreme of the nuclear landscape with ISOLTRAP](#) • [Studying short-lived radioactive molecules with CRIS](#)

Beta-decay studies • [Search for scalar currents in the weak interaction](#) • [Probing the structure of yrast states in even-even \$^{214,216,218}\text{Po}\$ through fast-timing measurements following the \$\beta\$ -decay of \$^{214,216,218}\text{Bi}\$](#) • [Electron capture of \$^8\text{B}\$ into highly excited states of \$^8\text{Be}\$](#) • [Shape coexistence in proton-rich \$^{182,184,186}\text{Hg}\$ isotopes studied through \$\beta\$ decay](#) • [Nuclear structure studies of exotic nuclei: the cases of \$^{31}\text{Ar}\$ and \$^{33}\text{Ar}\$](#)

RIB applications • [Effect of Cd doping on the local structure of vanadium oxides](#) • [TDPAC: A powerful tool to study \$\text{TiO}_2\$](#) • [Technical changes and updates on the On-line Diffusion Chamber \(ODC\)](#) • [Beamline upgrades and first biological studies](#)

Studies with post-accelerated beams • [A new triple foil plunger for lifetime measurements with MINIBALL/HIE-ISOLDE](#) • [Coulomb Excitation of Pear-Shaped Nuclei](#) • [A new frontier: direct reactions on nuclei below \$^{208}\text{Pb}\$ with \$N = 126\$](#) • [First measurements using the ISOLDE Solenoidal Spectrometer \$^{28}\text{Mg}\(d,p\)^{29}\text{Mg}\$](#) • [Halo effects in the low-energy scattering of \$^{15}\text{C}\$ with heavy targets](#) • [Shadow readout at the SEC](#) • [Beta decay of \$^{11}\text{Be}\$](#) • [Reaction with \$^9\text{Li}\$ at HIE-ISOLDE](#) • [\$^{11}\text{Be}\$ lattice location in GaN as function of temperature and doping type](#)

Other News • [MEDICIS Operation in 2018 and plans for LS2](#)

ISOLDE Support • [Support and Contacts](#)



Introduction

Gerda Neyens for the ISOLDE collaboration

2018 has been a very exciting year. The whole ISOLDE collaboration aimed at getting a maximum amount of experiments realized before going into a long 2.5 years of shutdown. More than 750 visits by members of the collaboration have been registered, to join a record amount of 51 experiments (532 shifts) that have been very efficiently scheduled by Karl between April 9 and December 3: 14 HIE-ISOLDE experiments and 37 low-energy experiments. Two of these experiments have been performed after the protons stopped on November 12, using long-lived Ra and Be isotopes that were extracted from earlier (cold) irradiated targets at MEDICIS.

The year started with the successful move of the 4th HIE-ISOLDE cryomodule (CM) from SM18 to the ISOLDE hall — see Fig. 1 — on January 23. This brings HIE-ISOLDE to its maximum achievable energy of 9.2 MeV/u for ion species with $A/Q=4.5$ (typical for heavy beams in the Pb region). Lighter ions having a lower A/Q can reach higher energies, up to 12.4 MeV/u for $A/Q=3$. After the commissioning with stable beams, first radioactive ion beams (RIBs) were accelerated on July 9.



Figure 1: Transport of the 4th Cryomodule

Thanks to an early start, we had a total of 31 weeks or 217 days of protons for ISOLDE (only 1 week less than last year). Low energy physics started on

April 9 and ran throughout the year until November 12. Thanks to occasional parallel operation of beams from GPS with beams from HRS, 36 low-energy experiments could be scheduled. At the end of the running period, several "proof-of-concept" experiments took beam in parallel/alternatingly, providing very important data to prepare for future new proposals. From July 9 onwards, priority was given to HIE-ISOLDE experiments: although protons stopped 1 month earlier than last year, Karl managed to schedule 13 HIE-ISOLDE experiments by grouping them in "blocks". A campaign of six successful Coulomb excitation experiments ran at Miniball during the summer, for which nine (!) different radioactive beams were accelerated to typically 4 to 5 MeV/u. This was followed by seven higher-energy reaction experiments using the full accelerator capacity and all three HIE-ISOLDE beam lines: two Miniball experiments with T-REX, one experiment behind and two inside the scattering chamber, and two experiments in the successfully commissioned ISS (Isolde Solenoid Spectrometer) with an array of Si detectors sent from Argonne National Laboratory (thanks for that). Also five stable beams were accelerated to different energies, and sent to ISS and Miniball for calibrating their systems. Thus, a record amount of 24 different isotopes were accelerated successfully this year, thanks to the very efficient work of the whole HIE-ISOLDE team! The highest energy reached with HIE-ISOLDE was for the ^{28}Mg beam accelerated to 9.5 MeV/u, which was sent to ISS at an intensity of $3.5 \cdot 10^6$ pps to study very successfully single particle levels in ^{29}Mg using the $^{28}\text{Mg}(d,p)$ reaction. Due to field emission issues in some of the rf-cavities, as well as a non-functioning cavity in the last installed cryomodule, the accelerator was operating this year at 75% of its nominal capacity. A few weeks ago, CM4 has been brought back to SM18 where its cavities will be repaired/replaced. When back

in place early 2020, this should bring HIE-ISOLDE to 85% of its nominal capacity at the start of the new running period. Further interventions on the cavities in other cryomodules will be discussed for the following YETS (Year End Technical Stops) in 2021 and beyond.



Figure 2: 4 Cryomodules installed at ISOLDE: February 2018

A very successful winter physics program was scheduled after the protons stopped on November 12, with two approved experiments that could run with long-lived radioactive beams from targets that had been irradiated a few weeks/months before at MEDICIS. Initially two HIE-ISOLDE experiments (with ^7Be and ^{44}Ti beams) and one CRIS experiment (with $^{223,224,225,226,228}\text{Ra}$ beams) were planned. However, due to uncertainties on the ion-source efficiency for the ^{44}Ti production, the latter was finally not retained.

This gave the opportunity for the CRIS experiment to continue its search for unknown transitions in RaF molecules during more than 10 days, yielding much awaited experimental information on their molecular spectroscopy, and even hyperfine spectroscopy.

An overview and preliminary results from the many successful experiments can be found in this newsletter.

Thanks to the excellent research performed by our collaborations, ISOLDE is becoming more and more visible at CERN. Your contributions for news items on the "CERN News" webpage and in the CERN Courier are highly appreciated (contact me or Karl if you want to announce a publication or a special realization). If you type "ISOLDE" or "HIE-ISOLDE" in the tag field of the website, seven contributions appear for 2018. There was a press release for the publication of the Hg odd-even staggering in Nature Physics, and six news items on a variety of topics (HIE-ISOLDE reaching completion, studying DNA with beta-NMR, mass measurements of Cr, PUMA). ISOLTRAP had two contributions in the CERN Courier (Jan/Feb and Jul/Aug). A report on our very successful ISOLDE Workshop and Users Meeting with a record of 156 registered participants appeared in this year's 1st issue of the courier (available on-line: <https://cerncourier.com/cern-courier-digital-edition/>).

We organized the EMIS Conference in September. It was attended by close to 180 participants from 20 countries and 60 institutes around the world. Many thanks go to our local fellows and PhD students, who took care of all practical organizational aspects. The next edition will be in Korea where we hope to see the first buildings from the new facility (RAON).

In January 2019, we had 1023 shifts remaining to be scheduled at ISOLDE. Some of those experiments have been approved many years ago. Therefore, the INTC meetings in 2019 will be devoted to revising the physics cases of all experiments. All spokespersons have been contacted to express interest in keeping or not their experiment active. As a result, we have now (April 2019) 776 shifts for which the physics case has to be re-evaluated. This will be an intensive process,

which we hope to finish by February 2020 latest. Calls for new proposals will then follow from spring 2020 onwards.

Finally, ISOLDE visits: we observed again an increase in the number of guided tours at ISOLDE, with more than 50 group visits (more than 1600 persons) and several VIP visits (more than 130 VIP's), as well as some professional and personal visits. The num-

ber of visitors increased from about 1550 last year, to nearly 1900 this year (and nearly tripled over the past five years). All this would not be possible without the excellent coordination work by Hanne Heylen, and the help of all the local ISOLDE people (physicists, engineers, ...). Thanks a lot to all of you for your continued support.

Gerda Neyens

ISOLDE Users Information

ISOLDE during LS2

During LS2 there will be no proton physics at ISOLDE. Many upgrades are underway most notably of the two front ends which will be replaced during this shutdown. The removal of the GPS and HRS frontends has been completed in March 2019 and the replacement works will continue until early 2020. Construction of the new nanolab for the production of nanostructured actinide targets will commence in late 2019. On the ISOLDE side various upgrades are taking place throughout the hall, especially around GLM/GHM which will be re-configured. There will be no beams from the separators in 2019 but it is hoped that stable tests will be possible in the second half of 2020.

On the INTC front a review of all experiments with outstanding shifts is underway with the first series of status reports being examined in the July INTC meeting. This will be followed by further status reports in November 2019 and February 2020. New proposals should be possible during 2020.

User registration for 2019

A full description of the procedure for registering at CERN is given at the end of the newsletter. Visiting teams should use the pre-registration tool (PRT) to register new users. As in 2018: the teamleader and deputy teamleader who sends the information via PRT must have a valid CERN registration. This also applies to

paper forms which have been signed at the visiting institute. If the teamleader or deputy do not have a valid registration, the users office will refuse to accept the documents.

Access to ISOLDE: ADAMS

Access to ISOLDE is now entirely managed through **ADaMS** (Access Distribution and Management System). For the uninitiated and experienced user alike, ADaMS can be quite confusing. The access permission required for ISOLDE is **ISOHALL**. Once submitted it will be sent for approval to the physics coordinator where training ranks will be checked before access is granted.

Required training courses for access to ISOLDE hall and chemical labs

There are a variety of training courses required before access to the ISOLDE hall can be granted. These are divided into hands-on courses, which take place at the CERN training centre in Preveessin, and online courses which can be taken via CERN online training.

New since last year's newsletter has been the migration of all training to the new CERN learning hub, lms.cern.ch, which replaces the sites cta.cern.ch and sir.cern.ch.

Enrollment for courses should take place for these courses in advance of coming to CERN; in the event that a user is not yet registered an email can be sent

to safety training: safety-training@cern.ch. However, once registered it will still be necessary to register for the hands-on courses in EDH in order to validate the training.

During LS2 the weekly training courses are not taking place as regularly as when physics is running. The physics coordinator will on occasion give special training courses to those who are unable to attend the normal training so that access can be granted. Please inform us as soon as possible of when this might be required.

- Pre-requisite online training courses (can be followed prior to arrival at CERN, if you are already a registered CERN user)
 - Mandatory courses for everybody:
 - * Emergency evacuation
 - * Radiation Protection - Awareness
 - * Safety at CERN
 - Electrical Safety Awareness - Facilities
 - Electrical Safety Awareness - Fundamentals
 - Radiation Protection - Supervised Area
- Required hands-on courses
 - ISOLDE - Experimental Hall - Electrical Safety - Handling
 - * Course code: STELS05IE
 - ISOLDE - Experimental Hall - Radiation Protection - Handling
 - * Course code: STIRP06IE
 - B. 508 chemical labs: The laboratories on the ground floor of 508 where solid state physics perform chemistry also have their own access. It is required to follow the online SIR course "Chemical Safety Awareness" before requesting the permission **ISOCHEM** for 508 R-002 and **ISOEXP** for 508 R-008 for the measurement area.

Visits to ISOLDE

Visits to ISOLDE are still possible. A typical visit consists of an overview presentation in the visitors' area in building 508 and, when possible, a tour of the ISOLDE facility itself along the pre-arranged visit path. In the event of a machine intervention or a conflict with physics which happens to be running, the tour of ISOLDE may be cancelled, and one remains in the 508 gallery area. Please note that weekend visits of groups are no longer possible and are not advised for individuals except in exceptional circumstances.

All visits are coordinated by Hanne Heylen (hanne.heylen@cern.ch) and she should be contacted well in advance with your wishes.

CERN open days: September 14 and 15 2019

This year CERN will host two open days where many experiments which are normally off-limits can be seen by the general public. ISOLDE will also feature for the first time with demonstrations and explanations taking place upstairs in building 508. For those interested in attending the open days, full information can be found [here](#).

ISOLDE Publications

Please note that ISOLDE should be mentioned in the abstract of articles related to experiments performed at the facility and, if possible, the ISOLDE team should be mentioned in the acknowledgements. Experiments which have benefited from ENSAR2 funding at ISOLDE must also mention this in the acknowledgements of any articles which emerge and which should resemble the following: *This project has received funding from the European Union's Horizon 2020 research and innovation programme under grant agreement No 654002*. Furthermore, please note that **all** publications which have received ENSAR2 funding are open access. This can be either green or gold but at the very least green open access will be expected of all publications which have received EU funding. Green open access can be fulfilled by submitting a manuscript copy of a paper to the CERN library following publication.

Publications on CDS

It is increasingly important that papers from ISOLDE

have proper visibility at CERN. To facilitate this, there is a specific area of the CERN Document Server from which all ISOLDE spokespeople and contacts will be able to upload DOI links (and extra information if required). Once you have signed in with your CERN credentials, you should be able to upload any new articles or theses. The link can be found [here](#). If there are any problems with uploading, please contact the physics coordinator.

ISOLDE papers as CERN preprints

It is now possible for ISOLDE papers to be uploaded to the CERN EP preprint server, which will allow the papers to receive a CERN-EP number as is the case for other experiments at CERN. The submission procedure can be found [here](#) and details about the format required are [here](#). Please note that these papers have to be approved beforehand, they should be sent to the physics coordinator who will assist with the process.

Safety in the ISOLDE hall

The wearing of safety helmets and shoes is mandatory inside the ISOLDE hall. It is also mandatory to check yourself on the hand-foot monitor before leaving the ISOHALL zone.

Once within the ISOLDE hall you have at your disposal additional protective equipment such as gloves and contamination monitors to ensure your safety. These are located in the cupboard close to the old control room.

A variety of "expert" courses are available for those required to perform more demanding operations such as those involving cryogenics, using the crane and lasers. Please ensure that you have followed these courses before performing these tasks.

For those performing electrical work (e.g. preparing cables, putting up HV cages), a 3-day CERN course needs to be followed (all local physicists have followed it). If you require more information about this, please do not hesitate to contact the coordinator.

The mechanical workshop in building 508 is fully operational. If you wish to use it a document will need to be provided which signed is by your team-leader, yourself, and our workshop supervisor, authoris-

ing you to use the selected machines in the workshop. For more information, please contact your experiment spokesperson, local contact or the coordinator.

The list of contacts for safety both for local experiments and visiting setups can be found at <http://isolde.web.cern.ch/safety>. All visiting setups should ensure that they have had a safety inspection before their experiment starts at ISOLDE. Please allow sufficient time for this to be done. You can contact the coordinator for more information to prepare for this.

Technicians for users at ISOLDE

ISOLDE still has as its disposal the services of two technicians — partly funded by the ISOLDE collaboration — who can assist with mechanical work and installation work for experiments during LS2. Their names are Francois Garnier (162968) and Antonio Goncalves Martins De Oliveira (163947). To request any work please contact the physics coordinator.

ORCIDs for researchers

ORCID (Open Researcher and Contributor ID) is a non-profit organization — partly funded by CERN — which is supported by a global community of organizational members, including research organizations, publishers, funders, professional associations, and other stakeholders in the research ecosystem, which has developed a unique researcher identifier that makes it easier to identify your publications. An ORCID account enables you to hold a record of all your research activities, variants of your name, affiliations, etc and is a unique identifier that can accompany you throughout your career, as affiliations, and sometimes also names, change.

CERN is encouraging all users to obtain an ORCID so as to remove any ambiguities which can occur for publications. Registration is relatively easy and generates a unique ID that you can use every time you publish a paper; the link to the ORCID website is [here](#). If you wish, you can add information about your affiliation and publications. You can also define whether specific data within your record will be private or public.

Removal and shipping of equipment from the ISOLDE hall.

All equipment which has been in the ISOLDE experimental hall requires a control by radiation protection before it can be transported elsewhere or back to home institutes. A new "buffer zone" has been installed in the

ISOLDE hall (close to the SAS and the HIE-ISOLDE tunnel) which implements the CERN-wide TREC system to ensure that all controlled equipment has traceability. This is now incorporated into the EDH flow for all transport requests from the ISOLDE hall.

ISOLDE facility

Target and Ion Source Development during LS2

Ferran Boix Pamies, Jochen Ballof, Joao Pedro Ramos, David Leimbach, Vasileios Samothrakis, Nhat-Tan Vuong and Sebastian Rothe for the ISOLDE TISD Team

The second Long Shutdown (LS2) of the LHC accelerator complex provides an excellent opportunity for the target and ion source development (TISD) teams to tackle the backlog of projects aimed at improving the overall performance of the target and ion source system. The selection of projects presented here includes thermal optimization of the targets, ion source designs, infrastructure upgrades, target material and molecular beam studies as well as last year's highlight: the on-line tests of the internal proton to neutron converter.

1 Proton to neutron converter

Neutron-rich fission fragments are currently of great interest for the physics community. These neutron-rich fission fragments are readily available at ISOLDE using the ISOL (Isotope Separator On-Line) method. However, if produced by direct irradiation (1.4 GeV protons) of uranium carbide (UC_x) targets, commonly used at ISOLDE, the desired isotopes come with very high isobaric contamination from neutron-deficient fission fragments. Since the year 2000 at ISOLDE, a tungsten/tantalum spallation source has been positioned close to the UC_x target and irradiated instead. The produced spallation neutrons irradiate isotropically and interact with the target producing very high purity neutron-rich fission fragments. However, scattered protons from the bombardment of the tungsten (W) bar still hit the target causing the non-desired impurities.

An ISOLDE (p2n) converter design optimization has been proposed before [1] and a simplified version has

been tested under proton beam irradiation [2]. In both, the current and the tested prototype designs, the converter is put just below the target and is indirectly and actively cooled by water. In order to use the full solid angle of the emitted neutrons and have the highest possible neutron flux a solution has been studied where the W converter is positioned inside of the target. While this solution presents large gains in production rates and a slight increase in purity of the desired beams, it presents many engineering challenges. By positioning the W converter in the center of the UC_x target, normally operated at 2000°C or higher, a larger diameter target oven has to be developed. Furthermore the chemical compatibility between all the target/converter components has to be guaranteed.

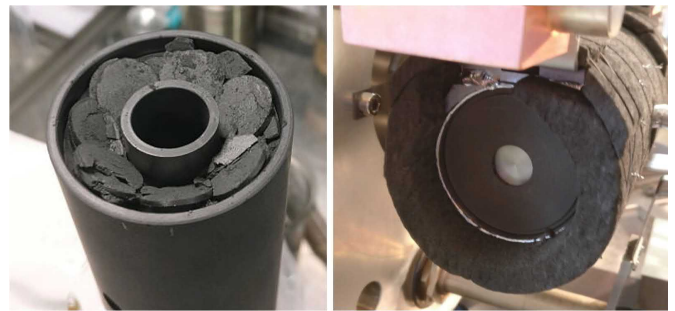


Figure 1: Left - filling of the graphite sleeve of the p2n-converter prototype with standard UC_x pellets; right - photo of the p2n-converter with special thermal shielding and target cap opened where the W bar can be seen inside of the UC_x containing graphite sleeve.

In addition from the 1.4 GeV pulsed proton beam - 2.8 kW (1.2 GW instantaneous, 2.4 μ s pulse length) - up to 700 W are deposited in the converter, while submitting the W to large power depositions in very short times. Since the converter sits inside the tar-

get oven, it also acts as an internal heat source for the target, which needs to be controlled with some precision to avoid target degradation and promote isotope release. To do such optimization studies, simulations on isotope production, power deposited (*FLUKA*) and thermo-mechanical aspects (*ANSYS*) of the target oven have been performed [3] and a prototype has been build (see Fig. 1) and tested online.

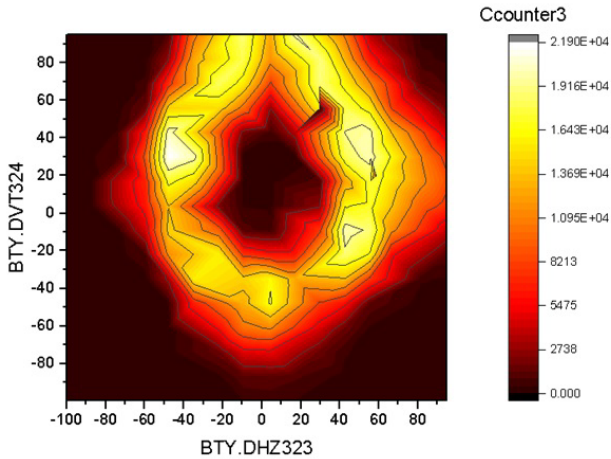


Figure 2: Proton scan of the p2n-converter prototype showing the vertical and horizontal proton beam deflectors and the count rates of ^{26}Na .

The prototype p2n-converter was tested online at the HRS separator [4], for about 10 shifts, at the end of the 2018 ISOLDE running period. More than 100 yield measurements were made by positioning the beam on the target and converter, to evaluate its performance. Due to its peculiar shape the so called 'proton scan' was done using the full deflector range and a plot was produced (see Fig. 2). The isotope ^{26}Na was used since it should be produced by bombarding the UC_x circular shape with protons, while when bombarding the W (center) there should be none. This converter is the first high-power target at ISOLDE, and its temperature has to be regulated accordingly to the proton beam intensity. By switching off the target heating and using $2\ \mu\text{A}$ of proton beam intensity on the converter brings the W rod up to about 1900°C which heats the UC_x to almost 1700°C . In total 7 elements were measured: the surface ionized Na, Rb, Cs and Fr (with ISOLTRAP assistance for the purity of Rb and Cs isotopes) and in collaboration with the RILIS team, laser ionized Ga, In and Zn. The data is currently under analysis, but exotic

isotopes such as ^{102}Rb and ^{150}Cs were seen in a few hundreds/s range while bombarding the converter.

2 Molecular Beams

The extraction of radioactive isotopes as molecular compounds (sidebands) has proven to be a powerful technique for thick-target ISOL facilities. Molecular sidebands are commonly used in two cases. Firstly the purification of beams from isobaric contaminants which may dominate the beam composition at the mass of the desired atomic species, rendering impossible physics experiments which require pure beams. Secondly the *in-situ* volatilization, in which non-volatile atomic radionuclides are offered reaction partners to form volatile carrier molecules. A prominent example of the former is the production of carbonyl selenide beams from zirconia fiber targets using a forced electron beam-induced arc discharge (FEBIAD) ion source [5]. Refractory element extraction has been successful in many cases, typically as a halide or oxide compound [6]. The most recent development was the extraction of boron as fluoride (BF_x , where $0 \leq x \leq 3$) [7]. While molecular beams significantly increase the variety and purity of available beams, the processes involved are more complex, and often lack a complete description. During the long shutdown period, we will launch an experimental campaign aiming at a better understanding of molecular beam formation. The outcome of the investigations will contribute to improvements of beam reliability, purity and yields.

We will build a dedicated setup to investigate underlying chemical reaction mechanisms and material compatibility, which can, for example, be used to tackle issues experienced with the stability of carbonyl selenide beams [8]. The majority of experiments will be performed using the ISOLDE offline separator facilities, which are equipped with an analyzing dipole magnet, allowing the Faraday cup measurement of m/q-separated beam. However, the mass resolving power of the device is limited and does not allow isobaric molecular species to be identified.

With FEBIAD type ion sources, which are capable of ionizing elements with high ionization potential, complex mass spectra are obtained. The unambiguous assignment of peaks to molecule fragments can in some cases be challenging. Therefore we will investigate, if a more sophisticated characterization of the separated beam can be achieved by other means, for example through coupling an MR-ToF device to our off-line mass separator.

3 An off-line ion source

During LS2, extensive ion source studies are planned. This includes defining operational parameters, stress tests and development towards higher efficiency and selectivity of existing ion sources as well as exploring new ion source concepts. For this project, a dedicated ion source test stand, capable of extracting and monitoring the total ion beam from an ion source under test, has been developed.

As a spin-off application of this test-stand, a standalone negative ion source for photodetachment studies of negative ions, shown in Fig. 3 is in development. Here, a tubular lanthanum hexaboride (LaB_6) surface ionizer is used to create negative ions. Initial tests of the source geometry have been performed at the offline 1 mass separator and the ion extraction optics have been conceived and constructed.

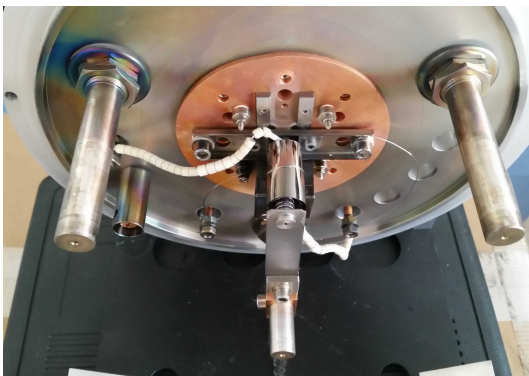


Figure 3: Offline ion source for negative ion studies. A lanthanum hexaboride tube is externally heated by a heating coil. A mass marker with the desired ion species can be inserted in the back and is heated separately.

As a next step, mass separation capabilities via, for example, a QMF will be added, increasing the feasibility

of a variety of studies of different stable elements. By incorporating the ISOLDE target design, existing infrastructure such as the test stands and offline separators can be used.

Additionally, the development of such an off-line ion source creates synergies with various experiments at ISOLDE, most of which use or are planning to use an off-line ion source for beam tuning and initial setup.

4 Upgrades of the RF and gas delivery system to ISOLDE targets

The ISOLDE front-ends (FE) located at the GPS and HRS mass separators deliver a number of services to the exchangeable targets: electric current for heating of line and target, electric potentials for FEBIAD ion sources, water cooling, thermocouple connections, gas supply and radiofrequency signals. The combination of all these features provides the flexibility in target and ion source combinations which allows the production of a large variety of radioactive ion beams.

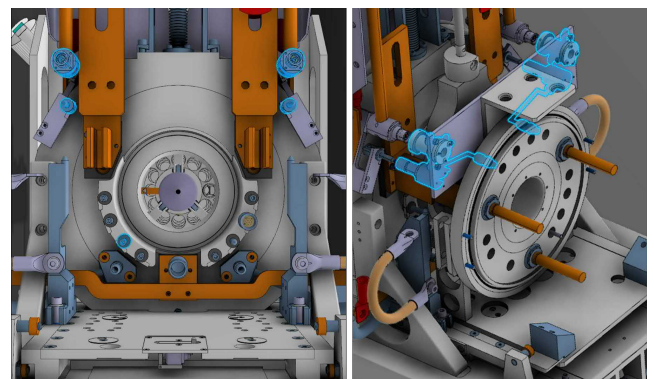


Figure 4: (Left) Front-end coupling table with new connections highlighted in blue. (Right) New target coupling plate for extra connections.

Within the exchange of both FEs planned for the beginning of LS2, the target services system for the RF and gas delivery will be upgraded. After, yet another, successful run in 2018 with the LIST (Laser Ion Source and Trap) [9], future experiments using this laser ion beam purification device will benefit from two RF signals available at both FEs: HRS and GPS. As a consequence, the signal-splitting transducer box that was attached to the target unit can now be suppressed,

which will simplify the design, ease storage and handling, reduce nuclear waste and avoid potential inter-ventions near the target. The LIST surface ion suppression can will now be available for Users requiring the higher mass resolution of the HRS and/or the ISOLDE cooler buncher (ISCOOL).

As a second modification, two additional gas connectors will be available, allowing for chemical purification of the FEBIAD ion source buffer gas and eventually gas circulation in the targets [10]. These extra features open the path for future applications to control chemical formation of volatile species in the target, key for the production of RIBs of refractory elements.

5 Improving the target and ion source heating

One goal of current target development aims at an improved temperature homogeneity across the target container, the transfer line and the ion source, avoiding cold spots which are detrimental to the extraction efficiency, especially for short-lived isotopes.

As a first step, the current ISOLDE target/ion source heating system was investigated: an ISOLDE target with an MK1-Ta surface ion source and the standard thermal insulation (metallic thermal screens) was heated to a maximum of 2000°C (target container to 570 A, line to 260 A). The temperature was measured at 6 points along the ion source and transfer line using a pyrometer through holes drilled in the thermal insulation screens.

A large temperature difference of $DT=613^{\circ}\text{C}$ between the flexible line connection and the center of the hot cavity was observed. To mitigate this, it was proposed to a) reduce the cross-section of the connecting lead and to b) move the connection to the back of the transfer line. A prototype container with the line heating lead welded to the back of the transfer line and a classic container have been prepared (c.f. (1),(2) in Fig. 5) and the thermal profiles were measured under the same heating conditions. A special target lid with

viewports allows optical access in many directions. In both cases the thermal screens were omitted to facilitate the measurements with the pyrometer and to simplify the corresponding electrothermal simulations. The results are shown in Fig. 5. It is clearly seen that the prototype design has an improved thermal profile.

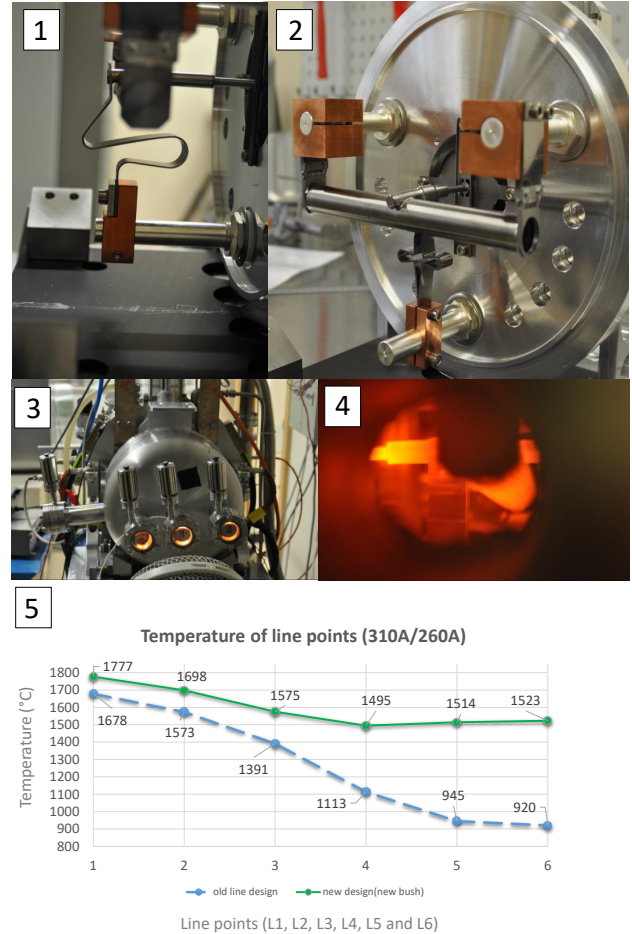


Figure 5: 1) Prototype with the line connection at the back 2) Current version with the line connection at the front 3) Casserole with special windows so as to be able to measure the temperature at the different line points 4) View from the window while target is heated up 5) Temperature comparison of the six line points between the two prototypes.

A complementary development aims at improving the thermal screens. To date, the heat screens are built from 5 layers of Ta, W and Mo sheets, manually cut in shape and carefully wrapped and fixed around the target containers. This solution impacts the assembly time and has limited reproducibility. At high temperatures and over time, the shielding efficiency can decrease leading to a deviation of the temperature calibration. Alternative materials such as *Sigratherm*[®] MFA carbon foam or ceramics like ZrO_2 that can be shaped specif-

ically, thus enabling tailoring of the desired temperature profile are currently investigated. The superior heat screening efficiency of *Sigratherm® MFA* foam was already demonstrated on-line with the internal p2n converter and at the MEDICIS target container with their large diameter containers (see section 1).

sides of the target container and the plug at the end of the transfer line.

6 Optimization of the uranium carbide production

Highly porous and refractory uranium carbide (UC_x) target materials are used in more than 60% of ISOLDE targets. UC_x is produced at the ISOLDE class A laboratories by heating pellets composed of a mixture of UO_2 and excess graphite up to 2000 °C under high vacuum.

During the process, the temperature is progressively increased while the pressure is kept below 2×10^{-4} mbar. The carbothermal reduction of the UO_2 follows the chemical reaction $UO_2 + 6 C \rightarrow UC_2 + 2 C + 2 CO$ at temperatures >1000 °C. This phenomenon is accompanied by a pressure increase in the reacting vessel due to the release of CO. As the temperature is progressively increased, the sintering of UC_x occurs possibly causing the collapse of pores of small dimensions [11]. While the carbothermal reduction process can easily be monitored by observing CO production, the microstructure evolution has never been fully characterized at CERN.

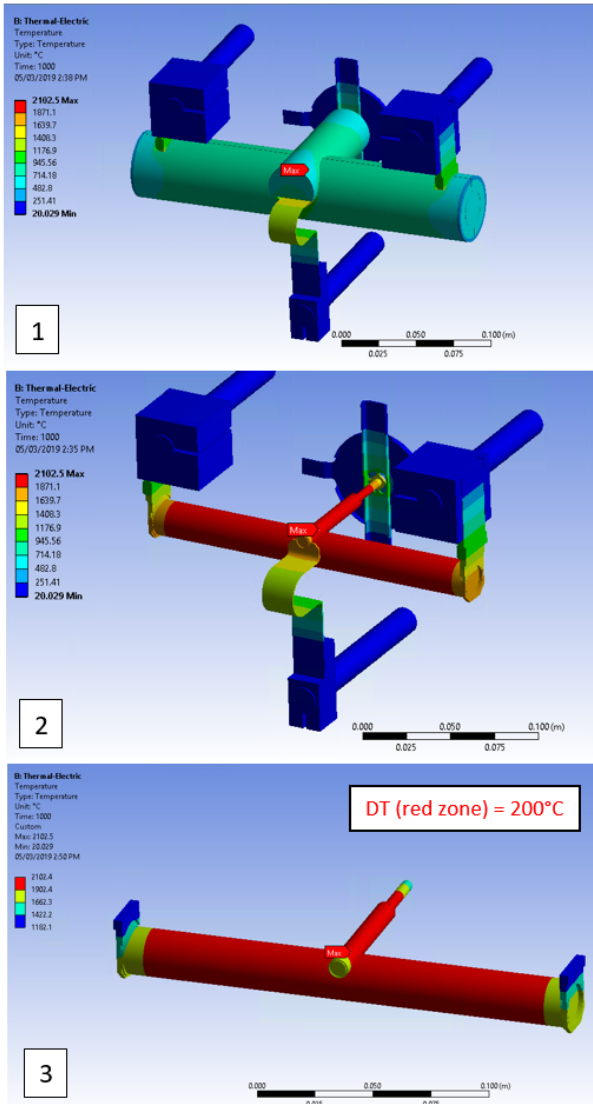


Figure 6: 1) Temperature profile of the target with the thermal insulation visible in ANSYS 2) the same with the thermal insulation hidden 3) Temperature profile of the container and the line clearly showing the cold spots at the target heating connections and the plug of the transfer line.

In the next step a prototype with the line heating connected at the back and carbon foam as a thermal insulation material will be tested. This version has been simulated in ANSYS Workbench and gives very promising results for the improvement of the efficiency of ISOLDE targets, the results are shown in Fig. 6. After this we will address the cold spots found in the two

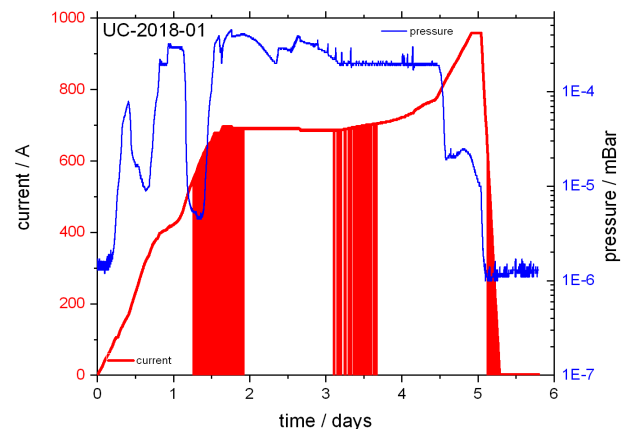


Figure 7: Example of heating current and pressure vs time during the production of a UC_x batch in 2018.

The current UC_x production method takes on average 5-7 days to complete. A recording of the pressure and the heating current over time is shown in Fig. 7.

During LS2, we aim to fully characterize the UC_x

production process and we will try to reduce the production time while maintaining the same microstructural characteristics. For this, small test batches will be produced at different pressures and different heating rates. The porosity of the resulting UC_x will be measured by gas adsorption analysis (BET) and under a scanning electron microscope (SEM). As a second stage, samples will be kept at operating temperatures for extended periods, allowing us to monitor and eventually model the sintering process.

7 An oxidation process for irradiated uranium carbide targets

Each UC_x target is operated on average for 1-2 weeks at ISOLDE. Due to its pyrophoric nature, UC_x requires extreme care in all handling procedures and it is therefore unsuitable for long-term storage in this form.

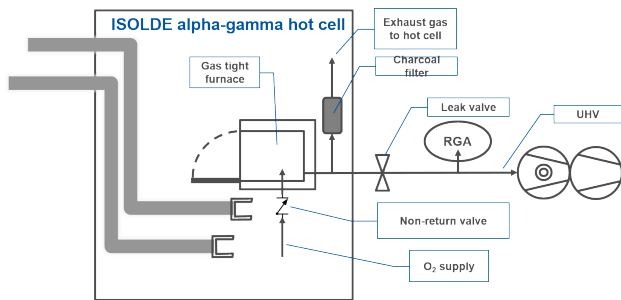


Figure 8: Schematic of the future UC_x oxidation set-up in the ISOLDE alpha-gamma hot cell.

Investments in thermal analysis instruments have been made to investigate a safe and efficient process for the conversion of UC_x into U_3O_8 on a laboratory scale. A set-up for the stabilization of irradiated UC_x target material will be designed and installed

in the ISOLDE alpha-gamma hot cell during LS2. A schematic view of the oxidation station is shown in Fig. 8. The procedures developed here could be transferred to other facilities worldwide, as a new waste disposal channel.

References

- [1] R. Luis, J. G. Marques, T. Stora, P. Vaz, L. Zanini, *EPJ A* **48**(6) (2012).
- [2] A. Gottberg, *et al.*, *NIM B* **336**, 143 (2014).
- [3] J. P. Ramos, *et al.*, 'The design and tests for the new CERN-ISOLDE spallation source: an integrated tungsten converter surrounded by an annular UC_x target operated at 2000 °C', in review, to be published.
- [4] J. P. Ramos, *et al.*, to be published.
- [5] U. Köster, *et al.*, *NIM B* **204**, 303 (2003).
- [6] U. Köster, *et al.*, *NIM B* **266**(19-20), 4229 (2008).
- [7] J. Ballof, *et al.* (2019), Radioactive Boron Beams Produced by Isotope OnLine Mass Separation at CERN-ISOLDE, accepted for publication in *Eur. Phys. J. A*.
- [8] K. Chrysalidis, *et al.* (2019), Developments towards the delivery of selenium ion beams at ISOLDE, to be submitted.
- [9] D. Fink, *et al.*, *NIM B* **317**, 417 (2013).
- [10] J. Ballof, *et al.*, 'Experiment proposal to study transition metal carbonyl beams at isolde' (2018), <https://edms.cern.ch/document/2036665>.
- [11] L. Biasetto, *et al.*, *Journal of Nuclear Materials* **404**(1), 68 (2010).

RILIS operation and development: recent accomplishments and future plans

*Shane Wilkins, Katerina Chrysalidis, Bruce Marsh
for the RILIS collaboration*

The Resonance Ionization Laser Ion Source (RILIS) at ISOLDE continued its status as the most frequently used ion source at the facility in 2018, providing laser-ionized beams of 14 elements over 20 experimental runs. This includes laser-ionized actinium and scandium isotopes which were delivered to users for the first time at the facility. In total, 60% of the shifts at the facility utilized the RILIS last year.

To date, laser-ionized beams of 37 elements have been delivered with experimentally tested schemes available for an additional 17 elements. All information regarding ionization schemes can be found in the RILIS Elements Database which is continuously updated (link at bottom of contribution).

The RILIS infrastructure has also been used as a part of an extensive in-source spectroscopy program in the lead region with experimental campaigns on Au, Hg, Tl, Pb, Bi, and At isotopes since Long Shutdown 1. Numerous articles from these experiments have been published with 'Characterization of the shape-staggering effect in mercury nuclei' appearing in *Nature Physics* [1]. The technique was also used to study Dy ($Z = 66$) for the first time [2], investigating isotopes around $N = 82$. In addition to this, 3 electron photo-detachment experiments have been performed as part of the GANDALPH collaboration.

Multiple avenues are being pursued to expand the operational capabilities of the RILIS during CERN's Long Shutdown 2. New measures, allowing laser beams to be simultaneously stabilized inside both the HRS and GPS ion sources, will be implemented. This will remove one of the common operational bottlenecks that is encountered when performing parallel set ups and in some cases even allow dual-separator operation.

Work on commissioning the MELISSA laser labora-

tory is underway with the first laser-ionized beams at MEDICIS scheduled for May 2019. Additionally, a dedicated laser laboratory that will act as the hub for future RILIS developments at Offline 2 is currently being set up and will be home to a complete laser-ion-source installation. This will significantly reduce the current practice of 'parasitic' development during the on-line period at ISOLDE. Furthermore, the installation will act as a hardware backup in case of laser failures at the RILIS.

Significant investment has been made in narrow-linewidth laser systems to extend the RILIS spectroscopic capabilities. A narrowband injection-seeded Ti:sapphire laser was constructed, commissioned and successfully employed in the first Doppler-free 2-photon spectroscopy measurements at ISOLDE [3]. To improve the efficacy of the technique, work to investigate the optimal geometry of the mirror placed within the ion source will be undertaken. In addition to allowing the in-source spectroscopy technique to be extended to lighter mass regions, 2-photon ionization may allow the laser-ionized production of new elements and for a more universal isomer-selective mode of operation.

The use of a Raman laser for RILIS applications is being investigated with promising results already obtained using a diamond crystal as the active medium. The realization of such a system will allow the spectral range of the Ti:sapphire lasers to be extended into the blue-green region, removing the need for UV-pumped dye lasers.

References

- [1] B. A. Marsh, *et al.*, *Nature Physics* **14**(12), 1163 (2018).

<http://riliselements.web.cern.ch/riliselements/index.php>

[2] K. Chrysalidis, *et al.*, *NIM B: EMIS 2018 proceedings* (2019).

[3] K. Chrysalidis, *et al.*, *NIM B: EMIS 2018 proceedings* (2019).

Dielectronic recombination at REXEBIS

Hannes Pahl and Niels Bidault for the EBIS team

In an Electron Beam Ion Source (EBIS), successive electron impact ionisation is the main driver for increasing the charge state of the trapped ions. Charge exchange with residual gas and radiative recombination of beam electrons with the ions are prominent effects counteracting the charge breeding. The cross sections for these processes generally vary slowly with the kinetic energy of the electron beam. Opposed to this, Dielectronic Recombination (DR), which is the recombination of a beam electron with an ion while simultaneously exciting an ion-bound electron into a higher shell, is a resonant effect.

Due to its narrow resonances, DR is typically neglected when considering charge breeding dynamics. However, since the resonance energies depend on the element and the charge state of an ion, DR provides a way to manipulate the emerging charge state distribution in an EBIS through careful adjustments of the electron beam energy. If the resulting variations were strong enough, they could help to promote or suppress a given charge state during operation or serve as a diagnostic tool for the EBIS.

We have performed proof-of-concept experiments at REXEBIS using stable beams of $^{39}\text{K}^{1+}$ supplied by REXTRAP as well as continuous neutral gas injection of argon. The DR features were recorded by slowly varying the electron beam energy in the EBIS while monitoring the extracted ion current in several charge states using a Faraday cup behind the REX A/q separator. One of these scans, which were performed for a number of different electron beam currents and breeding times, is shown in Fig. 1.

Our measurements show that the relative strength of the DR features depends strongly on the electron

beam, because the natural linewidth (< 1 eV) of the DR transitions is smeared out by the energy spread of the electron beam ($\approx 20 - 50$ eV); a problem which becomes increasingly pronounced at higher electron currents. This suggests that only very strong DR transitions will be interesting for operational applications.

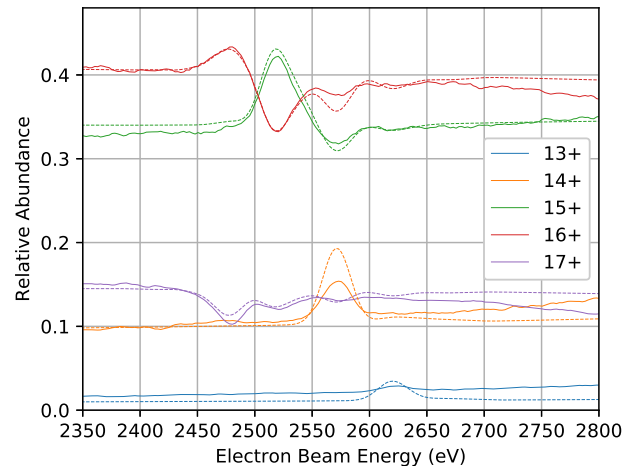


Figure 1: Measured (solid lines) and simulated (dashed lines) KLL-type DR features in the charge state distribution of ^{39}K for a charge breeding time of 900 ms at an electron beam current of 50 mA. When the electron beam energy matches a $n+ \rightarrow (n-1)+$ DR resonance, the abundance of the $n-1$ charge state is enhanced, while the charge states $\geq n$ are suppressed due to the increased recombination rate.

The measurements were guided by a charge breeding simulation toolbox which we developed in parallel to the experiments. The code solves a set of rate equations using established approximation laws for the cross sections of various processes and DR cross sections which were computed with the Flexible Atomic Code [1]. Fitting the model parameters results in a good match between the simulation (dashed lines in Fig. 1) and the experimental data and can yield some information about the EBIS performance. We plan to make this code available under a permissive license.

References

- [1] M. F. Gu, *The Astrophysical Journal* **593**(2), 1249 (2003).

Investigations for a future ^{11}C treatment facility Part I : Production

S. Stegemann and T. Stora for the MEDICIS-Promed team

The exploitation of light ions and PET isotopes such as ^{11}C for radio-therapy was proposed and tested long ago at the BEARS facility at LBNL. Since then, various facilities across the world came online for the post-acceleration of radioisotopes, mostly delivering radioactive ion beams (RIB) for nuclear physics [1]. Renewed interest in the exploitation of ^{11}C came when RIBs produced from ^{12}C fragmentation were used as low intensity pilot beams for imaging studies in small animal models in NIRS, Chiba. Within the MEDICIS-Promed ITN [2], we investigate new acceleration schemes to produce suitable RIB intensities of $4 \cdot 10^8$ ions/spill for hadron therapy with a focus on ^{11}C (β^+ emitter, $T_{1/2} = 20.4$ min) as it has excellent properties for both on-line and off-line PET imaging [3].

The implementation of a ^{11}C production system into existing hadron therapy centres faces challenges, e.g. the high beam intensity required for effective treatments. Taking these into account, the isotope production and post-acceleration method was identified as being a promising approach. The choice of the target is an essential criterion for the accelerator chain. In principle, many choices of beam energy - target combinations are possible, however only two types of targets are conceivable with respect to the production of high intensity post-accelerated ^{11}C beams. High-pressure N_2 targets (~ 20 bar) are commonly used for the production of ^{11}C for PET-imaging. In this method ^{11}C is produced in batch mode. The second possible approach to produce large quantities is using a solid, boron comprising target. Hence, a boron nitride (BN) ISOL-type target

was developed and characterized [4]. The target was manufactured to provide a controlled microstructure, for short diffusion- and effusion times to enhance its isotope release properties. First, the target was tested and characterized in various ways for optimization. The ^{11}C release efficiency was then experimentally measured in summer 2018 at CERN MEDICIS. BN pills were irradiated in the MEDICIS irradiation station position in a target especially designed for this purpose. Firstly, this design allowed it to be fully remotely manageable with the MEDICIS-MONTRAC and KUKA robot system. Secondly, it allowed easy and fast retrieval of the irradiated material for the experimental release study that followed, which was important due to the relatively short half-life. After retrieval, the activated material was transported to a class A laboratory within building 179 where the release study was performed. This study comprised a setup to determine the ^{11}C activity before and after a heat treatment by detecting the $\gamma - \gamma$ coincidences of the β^+ decay with two SpecMAT scintillation detectors [5]. This setup was designed to provide fast heating/cooling times to minimize losses during these processes. In this way, the ^{11}C release efficiency from BN targets, optimized for high intensity ^{11}CO beam production, was measured successfully for the first time. A preliminary analysis shows promising results. A more in-depth analysis is currently on-going.

References

- [1] T. Mendonca, et al., [CERN-ACC-NOTE-2014-0028](#).

- [2] '<https://cern.ch/medicis-promed/>'.
 [3] R. Augusto, *et al.*, *NIM B* **376**, 374 (2016).
 [4] S. Stegemann, *et al.*, Proc. of EMIS2018 (submitted).

ted).

- [5] '<https://fys.kuleuven.be/iks/ns/research/specmat/>'.

Investigations for a future ^{11}C treatment facility Part II : Charge breeding

F. Wenander for the MEDICIS-Promed team

We have also explored the possibilities of using a charge breeding system based on an EBIS for beam preparation of ^{11}C for acceleration with either a medical synchrotron or linear accelerator, and the complete results are presented in refs. [1, 2].

Injection into a medical synchrotron requires the EBIS to deliver a pulse of 10^{10} carbon ions within a pulse length of a few $10\ \mu\text{s}$. While it is straightforward to achieve a sufficiently short pulse length from an EBIS, the intensity requirement is very demanding. In combination with a medical synchrotron, it necessitates an EBIS with high electron beam current, which is, however, within reach of state-of-the-art technology. The real challenge is to efficiently store the radioactive ^{11}C during the synchrotron treatment cycle and to introduce it into the electron beam.

Tests have shown that a continuous injection into the EBIS can be excluded due to low efficiency and low output, as the EBIS cannot be filled properly to more than a fraction of its potential capacity. Using a Penning trap for collection can be ruled out as well due to its low capacity and inability to store C^+ ions for longer times.

To better exploit the space charge potential of the EBIS, the presently advocated solution is neutral gas injection via a cryogenic trap into the EBIS. In order not to fill the EBIS with background ion species, the target output could be purified, if required, either in a gas separation system or in an electromagnetic spectrometer after 1^+ ionization of the target gas.

In the case of a synchrotron treatment facility, a high-capacity EBIS with $1.3 \cdot 10^{12}$ electron charges, like

the RHIC EBIS, is required. For an all-linac facility operating with a high repetition rate of several 100 Hz, an EBIS equipped with a high-compression electron gun, such as the MEDeGUN, is more suitable. In this case a smaller electron space-charge capacity is sufficient due to the relaxed per-pulse intensity-requirements. In addition, it does not require the cryogenic trap as gas can be injected continuously due to the high repetition rate, making this the most favorable approach. Fig. 1 summarizes the viable scenarios.

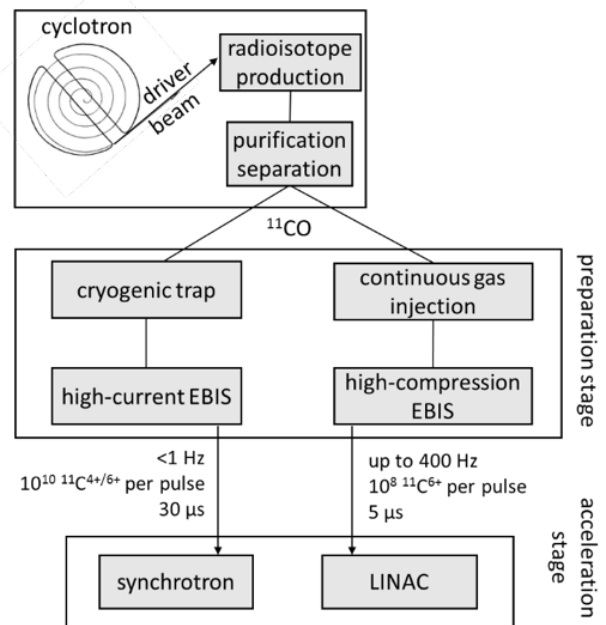


Figure 1: Summary of most promising approaches to ^{11}C acceleration. Figure taken from [1].

References

- [1] J. Pitters, *et al.*, CERN-ACC-NOTE-2018-0078.
 [2] J. Pitters, *et al.*, Proc. of EMIS2018 (submitted).

Challenges in using a pepperpot emittance meter

Fredrik Wenander for the EBIS team

Knowledge of the beam emittance is of importance for beamline, separator and accelerator design, but also for the setup of the experimental stations. In order to determine this one can use readily available pepperpot emittance meters (PPEM), but there are several secrets to master in order to perform measurements correctly. In ref. [1] we reveal some important aspects that need to be considered and may be of interest to the ISOLDE community.

We set out to measure the transverse emittance of multiply charged beams from REXEBIS with a PPEM [2] equipped with a Micro Channel Plate (MCP), a phosphor screen and a CCD camera for detection of the ion signal. The pulsed beam structure of low duty cycle imposed challenging constraints on the detector settings. Even though integrated particle intensities are relatively low, the instantaneous particle rates during the short pulse can be significant. The signal of the initial ion beamlet impinging on the MCP is transformed and amplified several times. First it is converted into an electron signal in the MCP and then in the phosphor screen into a light signal which is finally registered with a CCD camera and saved as a picture. In order to obtain absolute measurements it is crucial to ensure linearity in every single step, such that the intensity distribution of the ion beamlet is transformed linearly into a pixel intensity with no alteration of shape. The noise filtering is another important factor, and we present a method based on linear regression to zero noise threshold in order to minimize biased influence by the user. Finally, obvious errors stemming from limited transverse detector resolution and finite hole-size in the pepperpot, to more intricate sources, such as poorly adjusted camera focus and mixing between projected x/y planes due

to rotation of the camera with respect to the beamlet pattern, need to be under control.

RMS emittances of mass-separated beams after the REX separator range between 3 and 7 μm with a trend to higher values in the horizontal than in the vertical plane. The variation is due to scraping the REX separator line for different beams. The range of emittances agrees with previously determined values. The RMS emittance of a non-separated beam with an extraction potential of 35 kV was determined to be 4 μm , which is in accordance with theoretical predictions. For space-charge neutralized electron beams in the EBIS, the ion beam emittance increases significantly (a factor 3 for 65% neutralization), and the large-diameter beams suffer from spherical aberrations in the extraction system (see Fig. 1).

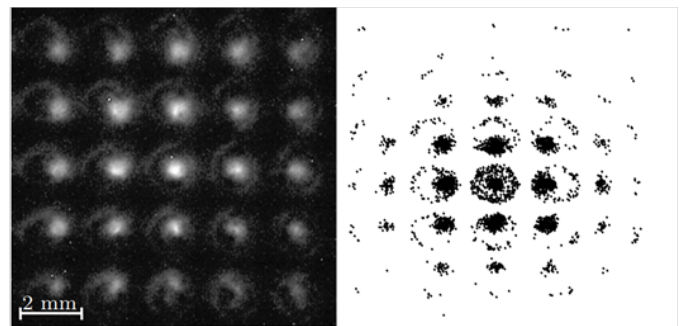


Figure 1: Left: Emittance picture at MCP plane (zoom) of a Xe beam at 67% space charge neutralization. Right: SIMION simulation of a beam passing through an Einzel lens (filling factor 60%) and a pepperpot mask. Picture taken from [1].

References

- [1] J. Pitters et al., *Nucl. Instrum. Meth. A* **922**, 28 (2019).
- [2] A. Pikin et al., *Pepper Pot Emittance Meter*, BNL Technote C-A/AP/244.

MEDeGUN - a high-compression electron gun for an EBIS charge breeder

Fredrik Wenander for the EBIS team

In general, it is a wish from the experiments of post-accelerated beams that the charge breeding time is reduced. In part to gain access to even shorter-lived radioactive ions, but mainly to enable operation of the linac at a higher repetition rate and thereby reducing the instantaneous particle rate impinging onto the detectors. For a few years we have been addressing this point by developing a high-compression electron gun, MEDeGUN [1], that is being tested at the TwinEBIS setup. The design is based on a combination of electrostatic and magnetic compression, which is commonly referred to as a Brillouin gun. The present electron gun at REXEBIS, a so-called immersed gun, is less complicated to build and commission but only makes use of magnetic compression and therefore the achievable electron current density is lower. MEDeGUN is actually foreseen to be used in an EBIS designed to act as a C^{6+} source for linac-based hadron therapy facilities, but would also serve the purpose in a charge breeder for radioactive ions.

The central gun geometry given in the Fig. 1, shows the electrostatic parts consisting of cathode, Wehnelt and anode electrodes, and the iron shield. The concave dispenser cathode is operated in the space-charge limited mode at approximately $1100^{\circ}C$. The water-cooled electron gun is axially moveable with respect to the magnetic field from the main 2 T solenoid. The alignment tolerances of the critical parts are less than $100\ \mu m$.

During the first commissioning run in early summer 2017, the design goals for the electron current and energy of 1 A at 10 kV acceleration voltage were already reached [2]. Since then the setup has undergone small modifications, and recent tests have proven stable and

reproducible operation also at lower, i.e. more difficult, beam energies, with vacuum pressures similar to the REXEBIS system.

We have also shown that a 1.5 A beam can be transmitted at 8 kV acceleration voltage. The high current at a moderate acceleration voltage result in a large trapping capacity of the EBIS, making this gun suitable for higher radioactive ion beam intensities expected from future radioactive beam facilities.

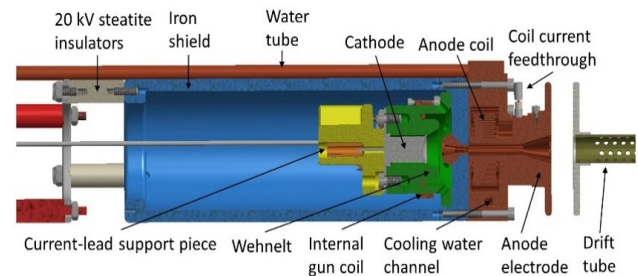


Figure 1: Cross-section of the electron gun assembly. The iron shield (blue) supports the Wehnelt piece (green), which in turn holds the cathode (grey). With the coils the magnetic field at the cathode and in the crossover point can be adjusted.

Even though the actual electron beam density has not yet been measured, it is expected that the charge breeding time of heavier elements could be reduced by a factor 10 if installed at REX/HIE-ISOLDE, while maintaining the breeding efficiency. The electron gun still needs to undergo long-term reliability tests, and its design should ideally be simplified if to be installed on-line.

References

- [1] R. Mertzig et al., *Nucl. Instrum. Meth. A* **859**, 102 (2017).
- [2] M. Breitenfeldt et al., *AIP Conference Proceedings* **2011**(1), 040004 (2018).

Ground-state properties

2018 at the Collinear Resonance Ionisation Spectroscopy (CRIS) experiment

Results of experiments IS639, IS620, IS613, and IS657

Ben Cooper for the CRIS collaboration

2018 was a busy year at CRIS. In April, laser spectroscopy of neutron-deficient indium isotopes from ^{101}In to ^{113}In was performed. This investigation, and others in the vicinity of ^{100}Sn and ^{132}Sn are designed to aid the understanding of the nuclear many-body problem. Recent developments in nuclear theory have also renewed the interest in this region of the nuclear chart [1, 2]. Later in the year we performed measurements on stable and neutron-deficient Sn isotopes yielding hyperfine structures, and isotope shifts of isotopes between ^{124}Sn and ^{104}Sn . A hint of a resonance in ^{103}Sn was also observed. In between these campaigns we measured the hyperfine structures of neutron-rich potassium isotopes up to ^{52}K . This experiment also demonstrated the efficacy of beta decay spectroscopy in combination with CRIS, which is a technique we will most certainly utilise in the future.

The development laboratory at The University of Manchester, where new techniques and apparatus are researched and tested, welcomed a strong new team including Miss Holly Anne Perrett, Dr Giles Edwards, and Dr Ben Cooper. This laboratory is currently leading the development of a new compact cooler buncher for injection of bunched ion beams into the CRIS beam line. The prototyping phase of this project is well underway and we envision significant gains in our data collection efficiency using such a device. It will give us the ability to utilise both separators at ISOLDE, optimise beam transport weeks in advance of an online campaign, and with integration of the ablation ion source [3] simplify the process of obtaining stable reference measurements.

Meanwhile, CRIS continues to collaborate actively with the University of Jyväskylä, where recent graduates from our collaboration (Dr Ruben de Groote and Dr Wouter Gins) continue to develop schemes of interest to high-resolution resonance ionisation spectroscopy.

In preparation for future experiments on radioactive molecules, stable-beam experiments on BaF were performed using an ablation ion source. A description of the laser and beam was published in October [3]. This prepared the CRIS experiment for the first laser spectroscopy experiment on a radioactive molecule. This successful final campaign before LS2 measured key spectroscopic properties of RaF which is a prime candidate for studies of fundamental symmetries and possible future EDM searches.



Figure 1: CRIS team members at our recent collaboration meeting.

References

- [1] T. Togashi, Y. Tsunoda, T. Otsuka, N. Shimizu, M. Honma, *Phys. Rev. Lett.* **121**, 062501 (2018).

[2] T. D. Morris, *et al.*, *Phys. Rev. Lett.* **120**, 152503 (2018).

[3] R. F. Garcia Ruiz, *et al.*, *Phys. Rev. X* **8**, 041005 (2018).

Determination of the electron affinity of astatine

Results of experiment IS615

David Leimbach, Julia Sundberg, Sebastian Rothe, Dag Hanstorp for the GANDALPH collaboration

Astatine, the purely radioactive element 85, is the rarest naturally occurring element on earth [1]. Its isotope ^{211}At is of interest for targeted alpha therapy (TAT), a method of treating cancer directly at the location of a tumor with alpha emitting particles [2]. However, some fundamental properties of astatine, such as its electron affinity (EA), the binding energy of the additional electron in its negative ion, are still unknown due to its scarce nature.

The EA, in combination with the previously measured ionization potential (IP) [3], gives valuable information for determining the chemical properties of astatine which are crucial for its application as an agent for TAT. Hence, the aim of the IS615 campaign was the determination of the EA of astatine. The experiment was performed with the Gothenburg ANion Detector for Affinity measurements by Laser PHotodetachment (GANDALPH), which was built in previous years and updated for the 2018 campaign. It comprises of an interaction region, a neutral particle detector and electrostatic beam optics. In the interaction region, the negative ion beam is overlapped parallel or anti-parallel with a frequency tuneable laser.

If the photon energy is equal or greater than the EA, the ion can be neutralized. Neutralized atoms impinge on a target where they create secondary electrons, which are detected by a secondary electron multiplier. By scanning the laser frequency around the threshold, the electron affinity can be obtained by fitting the data to the Wigner threshold law, which describes the cross section of the photodetachment process in the threshold region [4].

For 2018 and future campaigns, the neutral parti-

cle detector was equipped with a new target material, a graphene coated quartz plate instead of the previously used ITO coating. This decreased the background as well as increased the wavelength range of light into the UV wavelength region [5].

GANDALPH was connected to the GLM beam-line of ISOLDE where a negative $^{211}\text{At}^-$ beam with a yield of about $3 \cdot 10^6$ ions/s was delivered from a Th/Ta mixed foil target with an LaB_6 surface ionizer. This was sufficient to successfully perform the first measurement of the EA of astatine.

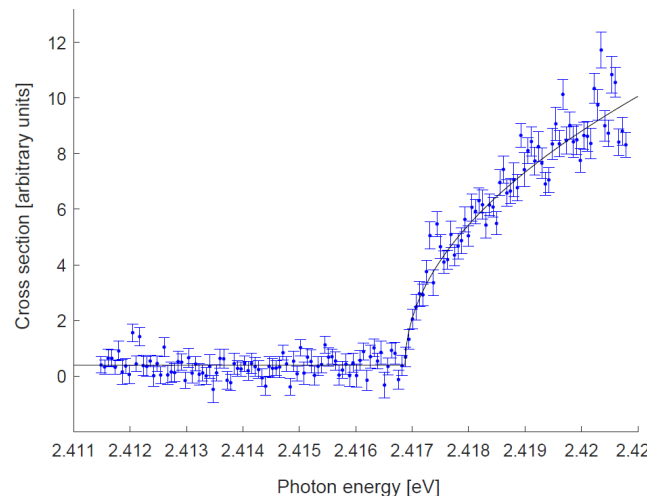


Figure 1: Photodetachment cross section of At^- . The figure shows data recorded using counter propagating laser and ion beams. The error-bars represent a 1σ statistical uncertainty and the solid line is a fit to the Wigner law.

In Fig. 1 the data from a single scan using counter-propagating laser and ion beams as well as the corresponding Wigner law fit is shown. The resulting value for the EA of astatine is close to the value of 2.412 eV, predicted by Borschevsky [6]. This successful campaign shows the feasibility of negative ion studies of radioactive elements only producible in minute quantities. This paves the way for the EA isotope shift studies in

chlorine (IS643) [7], which would give insight into the specific mass shift. Furthermore, the measurement of the EA's of polonium and the actinides is of interest.

References

- [1] I. Asimov, *J. Chem. Educ.* **30**(12), 616 (1953).
- [2] D. Mulford, *et al.*, *Journal of Nuclear Medicine* **4**(46), 199 (2005).
- [3] S. Rothe, *et al.*, *Nature Communications* **4**, 1835 (2013).
- [4] E. P. Wigner, *Phys. Rev.* **73**, 1002 (1948).
- [5] J. Warbinek, *et al.*, *Applied Physics Letters* (2018), submitted.
- [6] A. Borschevsky, L. Pasteka, V. Pershina, E. Eliav, U. Kaldor, *Physical Review A* **91**(2) (2015).
- [7] D. Hanstorp, *et al.*, 'Measurement of shifts in the electron affinities of chlorine isotopes', Tech. Rep. CERN-INTC-2017-053. INTC-P-515, CERN, Geneva (2017).

Laser spectroscopy on Ge isotopes across the $N=40$ subshell closure

Results of experiment IS623

*Anastasios Kanellakopoulos
for the COLLAPS collaboration*

The aim of IS623 is to provide electromagnetic moments and differences in the mean square charge radii of the ground states of the germanium isotopes ($Z = 32$) around the $N = 40$ subshell closure. One of our aims is to study the evolution of the small sub-shell effect observed in the nickel ($Z = 28$) and copper ($Z = 29$) charge radii [1] with increasing proton number. The germanium isotopic chain can also provide useful insight into the evolution of the inverted odd-even staggering effect, observed on the heavier krypton ($Z = 36$), rubidium ($Z = 37$), strontium ($Z = 38$) [2] and, most recently, gallium isotopes ($Z = 31$) [3]. By measuring the electromagnetic moments of the odd germanium isotopes, we can study the single particle and collective nature of their ground states, which are likely dominated by a hole/particle in three different single particle orbits around $N = 40$; a hole in $\nu f_{5/2}$ for ^{69}Ge , a hole in $\nu p_{1/2}$ for ^{71}Ge and one particle in $\nu g_{9/2}$ for ^{73}Ge . These moments can be compared with those of zinc isotopes [4]. The collinear laser spectroscopy technique (CLS) is an excellent method to study the moments and radii of Ge isotopes, yielding high-resolution results.

The $^{68-74}\text{Ge}$ isotopes were studied at the COLLAPS

beamline in May 2018. Neutron deficient and stable germanium isotopes are produced in a cold plasma ZrO_2 target with a sulphur leak. The sulphur binds with germanium into volatile GeS molecules, breaking apart inside the plasma source. The Ge^+ are then guided to the COLLAPS beam line, where the hyperfine structure of the atomic germanium is probed by the $4s^2 4p^2 \ ^3P_1 \rightarrow 4s^2 4p 5s \ ^3P_1$ (269 nm) transition after the charge exchange. The production of this laser frequency requires a blue or UV pump laser, which is no longer available in the COLLAPS laser lab. To close this wavelength gap, a frequency mixing unit (mixtrain) was installed, which allows us to generate the sum frequency of 824 nm laser light from our Ti:Sa laser and 1550 nm beam generated by a fiber laser. There, the two laser beams were superimposed and single-pass through a periodically poled crystal to generate the sum frequency at a wavelength of 538 nm. This light was then coupled into a frequency doubling unit to produce the second harmonic at 269 nm which was then sent to the beamline to be collinearly superimposed with the beam of atomic germanium.

Thus, for the first time the large hyperfine splitting of

the $4s^2 4p 5s^3 P_1$ atomic state of germanium was measured for $^{69,71,73}\text{Ge}$, a state sensitive to the nuclear electromagnetic moments.

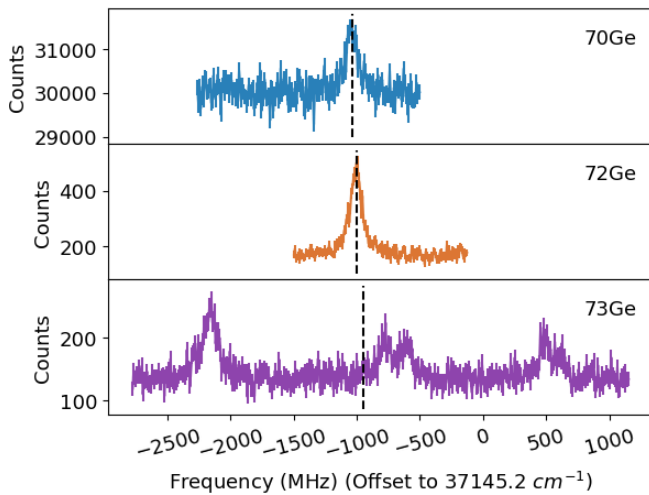


Figure 1: Hyperfine spectra for $^{70,72,73}\text{Ge}$. The isotope shift between the different Ge isotopes is visible despite being very small.

References

- [1] M. L. Bissell, *et al.*, *Physical Review C* **93**(6), 064318 (2016).
- [2] P. Lievens, *et al.*, *Europhysics Letters (EPL)* **33**(1), 11 (1996).
- [3] T. J. Procter, *et al.*, *Physical Review C* **86**(3), 034329 (2012).
- [4] C. Wraith, *et al.*, *Physics Letters B* **771**, 385 (2017).

Mass measurements of neutron-deficient indium isotopes at the extreme of the nuclear landscape with ISOLTRAP

Maxime Mougéot and Jonas Karthein
for the ISOLTRAP collaboration

Key in the establishment of the traditional concepts of nuclear shells, binding energy studies were also pivotal to the early realization of the demise of the traditional shell closures away from stability [1]. Extensive efforts have followed to assess the robustness of most major shell closures [2].

These studies now progress towards the $Z=N=50$ shell closures in close proximity with the proton drip-line. In 2018 a mass measurement campaign studied neutron-deficient indium isotopes in the vicinity of the doubly-magic ^{100}Sn . In the 2.5 days dedicated to the experiment, the online mass spectrometer ISOLTRAP was successful in measuring $^{99-101}\text{In}$. Figure 1 shows the yield of $^{99-101}\text{In}$ estimated from data of ISOLTRAP's Multi-Reflection Time-of-Flight (MRToF) device [3].

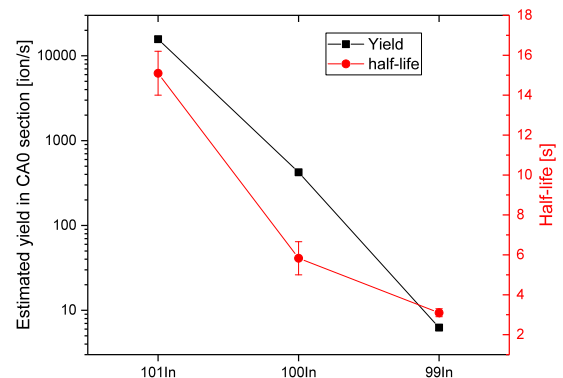


Figure 1: Estimated yields of $^{99-101}\text{In}$. Half-lives are taken from [4]. A LaC_x target with RILIS ionisation was used. The average proton current on target was $1.8 \mu\text{A}$ and the overall transport efficiency from the CA0 section was $\sim 0.3\%$.

While the successful measurements of ^{99}In and ^{100}In represented tough challenges for the now well established MR-ToF and ToF-ICR mass spectrometry techniques [3, 5], ^{101}In was measured with the

novel Phase-Imaging Ion-Cyclotron-Resonance (PI-ICR) technique [6]. It allowed for the separation of the ground and isomeric states in only 65 ms (see Figure 2). The estimated ground state to isomer production ratio is 25:1.

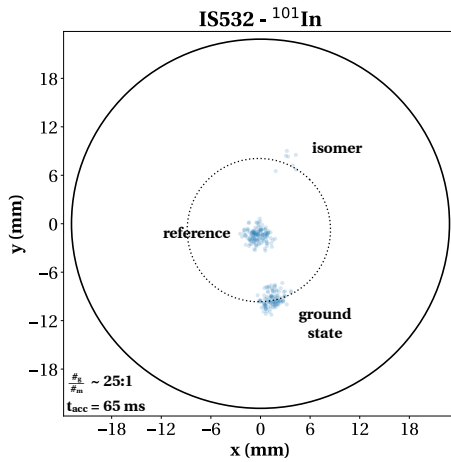


Figure 2: PI-ICR detector image showing the separation of the ground and isomeric states in ^{101}In . The reference spot marks the center of the circular motion.

This result constitutes the first determination of the

mass of ^{99}In and $^{101g,m}\text{In}$ while the uncertainty in the mass of ^{100}In (from which there exists a direct β -decay link to ^{100}Sn) is greatly reduced. The impact of these measurements for nuclear structure and rp-process calculation models are currently under investigation.

References

- [1] C. Thibault, *et al.*, *Phys. Rev. C* **12**(2), 644 (1975).
- [2] O. Sorlin, M.-G. Porquet, *Prog. Part. Nucl. Phys.* **61**, 602 (2008).
- [3] R. N. Wolf, *et al.*, *Int. J. Mass Spec.* **349**, 123 (2013).
- [4] G. Audi, *et al.*, *Chinese Phys. C* **41**(3), 030001 (2017).
- [5] M. Koenig, *et al.*, *Int. J. Mass Spec.* **142**(1), 95 (1995).
- [6] S. Eliseev, *et al.*, *Phys. Rev. Lett.* **110**(8), 082501 (2013).

Studying short-lived radioactive molecules with CRIS

Results of experiment IS657

R. F. Garcia Ruiz, S. G. Wilkins for the CRIS collaboration

In collaboration with theorists from quantum chemistry and experimentalists from different groups at ISOLDE [1], the CRIS collaboration measured, for the first time, the low-lying structure of several radium fluoride (RaF) molecules. To our knowledge, this is the first ever laser spectroscopy measurement of a short-lived radioactive molecule. This achievement constitutes a major step towards the study of radioactive molecules for nuclear structure and fundamental physics research. Some examples of low-resolution spectra measured for different RaF molecules are shown in Figure 1.

Certain molecular systems are ideal laboratories to probe the possible violation of fundamental symmetries and allow physics beyond the Standard Model to be explored with unprecedented sensitivity [2, 3]. Cur-

rently, precision measurements in molecules provide the most stringent constraints to the electron electric dipole moment (eEDM) [4]. As the degree of parity- and time-reversal violation effects scale with the atomic number, the nuclear spin and the nuclear deformation, molecules containing heavy (radioactive) nuclei are predicted to provide significantly enhanced sensitivity to these symmetry-violating effects [5, 6, 7, 8]. However, experimental measurements of such radioactive systems are scarce, and in most cases, quantum chemistry calculations constitute the only source of available information.

The complex structure of molecules, resulting from the additional vibrational and rotational degrees of freedom, vastly increases the number of states ($>10^4$)

that can be populated at a given temperature when compared to atoms. Moreover, radioactive molecules can only be produced in small quantities ($<10^7$ molecules/s), and their production and manipulation is not yet fully understood. Hence, their study requires particularly sensitive experimental techniques. The Collinear Resonance Ionization Spectroscopy (CRIS) experiment combined with the versatility of the ISOLDE facility offered a unique opportunity to perform this experiment. We hope that these results stimulate future collaborative efforts with new users at the facility in the search for new physics with radioactive molecules.

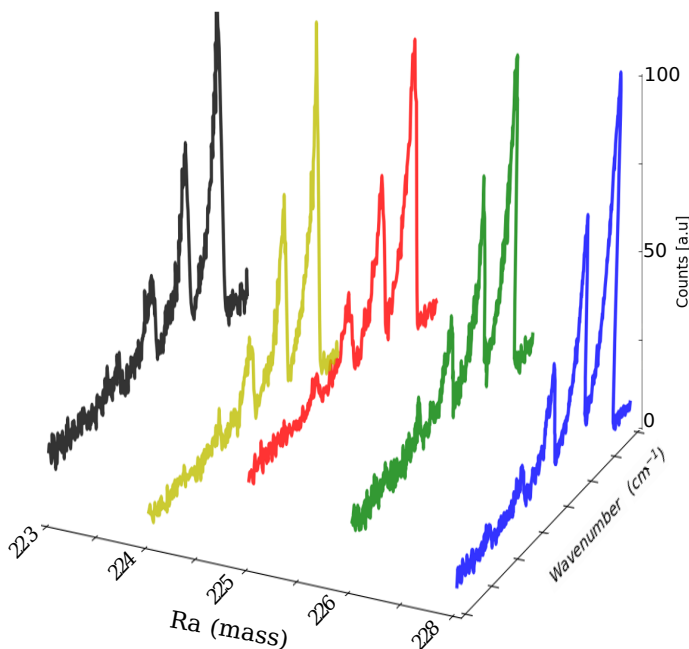


Figure 1: Low-resolution spectra of RaF molecules measured during the experiment. The low-lying spectra ^{223}RaF ($t_{1/2} = 11.4$ d), ^{224}RaF ($t_{1/2} = 3.6$ d), ^{225}RaF ($t_{1/2} = 14.9$ d), ^{226}RaF ($t_{1/2} = 1600$ y) and ^{228}RaF ($t_{1/2} = 5.7$ y) are shown with different colours.

References

- [1] R. F. Garcia Ruiz *et al* Collinear resonance ionization spectroscopy of RaF molecules *CERN-INTC-2018-017 / INTC-P-546*
- [2] V. V. Flambaum, D. DeMille, M. G. Kozlov Time-Reversal Symmetry Violation in Molecules Induced by Nuclear Magnetic Quadrupole Moments *Phys. Rev. Lett.* **113** 103003 (2014).
- [3] Emine Altuntas, Jeffrey Ammon, Sidney B. Cahn and David DeMille Demonstration of a Sensitive Method to Measure Nuclear-Spin-Dependent Parity Violation *Phys. Rev. Lett.* **120** 142501 (2018)
- [4] V. Andreev *et al* Improved limit on the electric dipole moment of the electron *Nature* **562** 255 (2018)
- [5] N. Auerbach, V. V. Flambaum, V. Spevak Collective T- and P-Odd Electromagnetic Moments in Nuclei with Octupole Deformations *Phys. Rev. Lett.* **76** 4316 (1996)
- [6] T. A. Isaev, S. Hoekstra, R. Berger Laser-cooled RaF as a promising candidate to measure molecular parity violation *Phys. Rev. A* **82** 052521 (2010)
- [7] A. D. Kudashov *et al* Ab initio study of radium monofluoride (RaF) as a candidate to search for parity- and time-and-parity-violation effects *Phys. Rev. A* **90** 052513 (2014)
- [8] V. V. Flambaum Enhanced nuclear Schiff moment and time reversal violation in ^{229}Th -containing molecules *Phys. Rev. C* **99** 035501 (2019)

Beta-decay studies

Weak interaction studies with β -delayed proton emission

Results of experiment LOI172

Dinko Atanasov for the WISArD collaboration

The search for physics beyond the standard electroweak model (SM) continues in many forms despite its remarkable success at the most elementary level. The reason to continue the search for new physics is the many yet unanswered questions by the SM such as the origin of parity violation. Furthermore, at the high-energy frontier, the Large Hadron Collider (LHC) could not find particles other than the Higgs boson which only set the limits to an even higher energy scale. [1] In this context, precision measurements at low energy provide the ideal case to study the existence of new types of the weak sector in a way that is complementary to the LHC. Currently, in the most general description of the beta decay Hamiltonian, besides Vector and Axial-vector terms, one finds Scalar and Tensor forms as well. The experimental limits on the coupling constants for the latter, from either neutron or nuclear beta decay, are on the level of a percent, not allowing one to exclude them completely [1]. Due to its sensitivity to both Scalar and Tensor interactions, the beta-neutrino correlation coefficient ($a_{\beta\nu}$) is a very attractive experimental probe which, if determined to a level of 0.1% (corresponding to a boson mass of the order of 2.5 TeV), might lead to the observation of deviations from the predictions of the SM, and hence new physics. It has been studied before at ISOLDE to a precision of a few percent, with results being in agreement with the SM [2].

The WISArD experiment (Weak-Interaction Studies with ^{32}Ar Decay) [3] is focusing efforts to determine $a_{\beta\nu}$ by using nuclei unbound to proton emission (such as ^{32}Ar), decaying in a strong magnetic field. The experiment relies on positron-proton coincidences to pre-

cisely determine the kinematic shift in the energy of the β -delayed protons emitted from the recoiling daughter nuclide. A proof of principle detection setup was installed in the fall of 2018, to study the super-allowed Fermi decay of ^{32}Ar ($0^+ \rightarrow 0^+$) to the Isobaric Analog State (IAS) in ^{32}Cl . The argon beam, delivered by ISOLDE, was transported and accumulated continuously on a 6 μm thick catcher foil situated in the center of the detection setup, where a 4 T external magnetic field was applied. This initial setup was comprised of one plastic scintillator (for positrons) and 8 silicon detectors (for protons). The proton detectors were divided into two groups and arranged in the upper and lower hemisphere of the catcher foil. Preliminary results from the experiment are shown in Fig. 1, where one can clearly see the different proton groups emitted after the β^+ decay, as well as the benefit of using coincidence measurements with the positrons. The complete dataset is still under analysis.

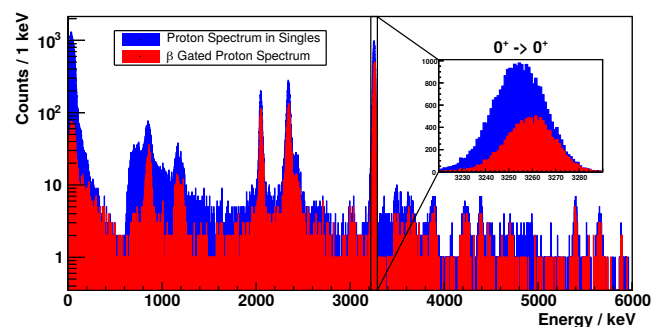


Figure 1: Proton energy spectrum from the decay of ^{32}Ar in singles (blue) and coincidence with the positrons (red) for one of the lower silicon detectors. In the inset, zoom on the super-allowed Fermi transition to the Isobaric Analog State in ^{32}Cl , presenting the kinematic shift due to the major vector current contribution.

References

[1] M. González-Alonso, O. Naviliat-Cuncic, N. Severijns, *Prog. Part. Nucl. Phys* **104**, 165 (2019).

[2] E. G. Adelberger, *et al.*, *Phys. Rev. Lett.* **83**, 1299 (1999).

[3] B. Blank, *et al.*, *CERN-INTC-2016* (2016).

Probing the structure of yrast states in even-even $^{214,216,218}\text{Po}$ through fast-timing measurements following the β -decay of $^{214,216,218}\text{Bi}$

Results of experiment IS650

Razvan Lica, Andrei Andreyev
for the IS650 and IDS collaborations

Nuclei in the vicinity of the doubly-magic $^{208}_{82}\text{Pb}_{126}$ represent crucial benchmarks for probing the predictive power of the nuclear shell model. In particular, Po isotopes having two protons above $Z=82$ are especially suitable for testing the seniority scheme across the long chain of isotopes, also spanning the $N=126$ shell closure. While extensive studies of 8^+ isomers in neutron-deficient even-even Po isotopes were performed in the past, not much is known about them in the neutron-rich cases. Such isomers can arise from several configurations, e.g. $\pi(h_{9/2})^2$, $\nu(g_{9/2})^n$, an α cluster coupled to a ^{208}Pb core or even from a mixture of them [1]. The lifetime measurements for the aforementioned 8^+ states (also for the other states of the yrast band, such as 2^+ , 4^+ , 6^+) provide important information on $B(E2)$ values for the respective γ -ray transitions, which can then be used to test the different theoretical approaches and underlying configurations. Thus, the goal of the IS650 experiment was to perform the first ever lifetime measurements of excited states in $^{214,216,218}\text{Po}$ via the fast-timing method following the β -decay of $^{214,216,218}\text{Bi}$.

The $^{214,216,218}\text{Bi}$ ions were extracted at ISOLDE from a standard UC_x target. After selective ionization by RILIS, the 1^+ Bi ions were accelerated by a 40 kV potential, mass-separated by HRS and finally implanted on the movable tape located at the center of the ISOLDE Decay Station (IDS). Almost pure beams of $^{214,216,218}\text{Bi}$ were obtained with intensities of $> 2 \times 10^4$, 1.5×10^3 and 2×10^2 ions/s, respectively. A β -gated

γ -ray energy spectrum recorded by the HPGe detectors is displayed in Fig. 1. It shows the clear identification of the γ -rays from ^{214}Po populated in the β decay of ^{214}Bi and the absence of other contaminants. The half-life measurement of excited nuclear states using the β - $\gamma(t)$, γ - $\gamma(t)$ and β - γ - $\gamma(t)$ fast-timing method [2] is a well established technique at IDS, covering a range of half-lives between 10 ps – 100 ns by employing fast-timing detectors such as $\text{LaBr}_3(\text{Ce})$ and plastic scintillators in coincidence with HPGe detectors. Preliminary results indicate a large discrepancy compared to the previous measurement of the reduced transition probability $B(E2; 8^+ \rightarrow 6^+) = 0.54(4) W.u.$ in ^{214}Po [1]. The analysis is currently on-going in order to establish the lifetimes of all yrast states in the $^{214,216,218}\text{Po}$ isotopes.

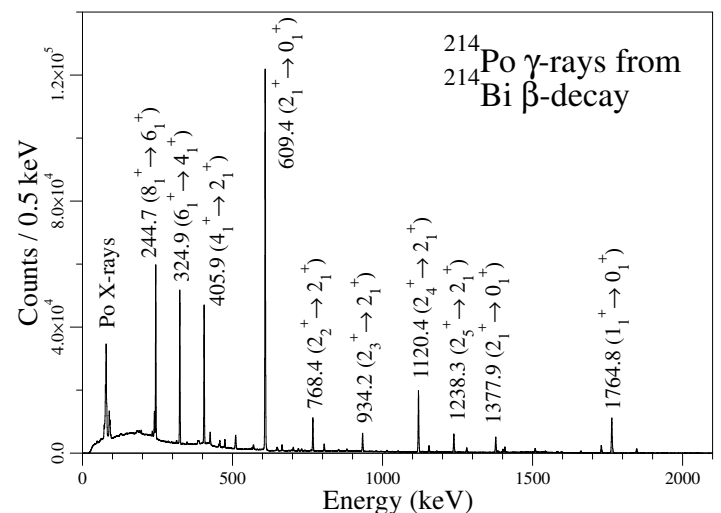


Figure 1: The HPGe β -gated γ -ray energy spectrum from the decay of ^{214}Bi .

References

[1] A. Astier, M.-G. Porquet, *Phys. Rev. C* **83**, 014311 (2011).

[2] H. Mach, R. Gill, M. Moszyński, *NIM A* **280**(1), 49 (1989).

Electron capture of ^8B into highly excited states of ^8Be

Results of experiment IS633

Silvia Viñals-Onses for the IS633 collaboration

The experiment IS633 aims to study the 2^+ doublet at 16.6 and 16.9 MeV excitation energies in ^8Be populated in the β^+ decay and electron capture (EC) of ^8B . In addition, we are interested in the so far unobserved EC-delayed proton emission from a state at 17.6 MeV. Assuming a factorization of the ^8B wave function into $^7\text{Be}+p$, an upper limit of the branching ratio to this state decaying into $^7\text{Li}+p$ is estimated to be 2.3×10^{-8} [1].

The experiment was divided into two parts. The first part was focused on the 2^+ doublet [2]. The second part of the experiment was dedicated to determining the branching ratio of the 17.6 MeV state ($\Gamma=10.7(5)$ keV) fed in EC and followed by delayed proton emission. The difficulty of this second part is two fold: the extremely low branching ratio and the low energy of the emitted proton, around 337 keV. In the following we discuss this second part of the experiment.

Description of the experiment

The availability of a boron beam at ISOLDE is very recent. The first positive test was done in 2015 with an estimated yield of ^8B of 10^4 ions/ μC . The beam was produced from a target made of pellets of multi walled carbon nanotubes and sent as a molecule to avoid the aggressive reactions of ^8B with other materials inside the target. The $^8\text{BF}_2$ beam ($A=46$) was implanted in a carbon foil (20 mg/cm²) inside of our chamber at the end of beamline LA1. The setup, shown in Fig. 1, was optimised to ensure an as background free spectrum as possible in the region from 200 to 400 keV. The average yield of ^8B was 2.5×10^5 ions/s. To cope with this huge yield a newly developed data acquisition system, *the shadowed multi-event readout* [3], was used in order to

maximise the data rate with minimised dead-time.

Ongoing analysis

By the use of anti-coincidence, the background in the region of interest is reduced by a factor of 10^3 . Fig. 2 shows the raw spectrum of the ΔE detector in blue overlaid with the anticoincidence spectrum in red.

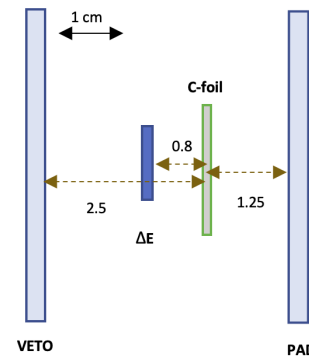


Figure 1: IS633 scheme for 2018 run: a thin ΔE detector of $30\mu\text{m}$ with negligible β -response. Opposite to it, a Si Pad ($3 \times \Omega_{\Delta E}$) to assure 100% coincidence coverage with ΔE . Behind the ΔE , a Si VETO with a large β -response.

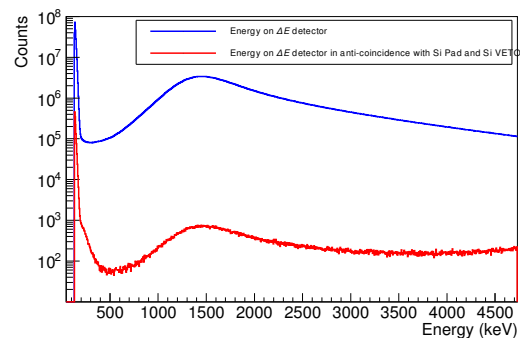


Figure 2: In blue, the raw spectrum (full statistics) obtained in the ΔE -detector is shown. In red, the resulting spectrum after applying the anti-coincidence with the Si Pad and Si VETO. Clearly the α and β responses are largely removed but there is still more analysis to be performed for a final result.

As can be seen in Fig. 2, a better algorithm to clean the spectrum in the region of interest is needed. So far we can only set an experimental upper limit for the branching to this state of 4.4×10^{-6} .

References

- [1] T. Nilsson, *Hyperfine Interact.* **129**, 67 (2000).
- [2] S. Vinals, *ISOLDE Newsletter* p. 22 (2018).
- [3] M. Munch, *IEEE TNS* **66**, 575 (2019).

Shape coexistence in proton-rich $^{182,184,186}\text{Hg}$ isotopes studied through β decay

Results of experiment IS641

Marek Stryczyk for the IDS collaboration

The proton-rich mercury isotopes represent one of the most prominent examples of shape coexistence [1]. The experimental γ - and electron spectroscopy studies point to the coexistence of two classes of states in the even-mass mercury isotopes with strong mixing between the low-lying states in $^{182,184}\text{Hg}$ [1, 2, 3]. In particular, the presence of strong $E0$ components in the $2_2^+ \rightarrow 2_1^+$ transitions are interpreted as a fingerprint for mixing between two states with different deformation [1, 3].

The spectroscopic quadrupole moments (Q_s) and monopole transition strengths ($\rho^2(E0)$), which allow states exhibiting different deformations to be distinguished unambiguously, will be measured in the Coulomb excitation (Coulx) experiment at HIE-ISOLDE [4]. However, additional spectroscopic information (branching ratios and internal conversion electron (ICE) coefficients) is needed for the data analysis [5]. Although these values have been provided by a previous thallium β -decay experiment [3], the uncertainties of the conversion coefficient and the γ -ray branching ratios for the $2_2^+ \rightarrow 2_1^+$ transition of interest are of the order of 20 – 30%. The main goal of the experiment was to reduce these uncertainties and, consequently, to increase the precision of Q_s and $\rho^2(E0)$ values in the future Coulx experiment.

The beams of $^{182,184,186}\text{Tl}$ were produced in proton-induced-fission of a UC_x target, selectively ionized by RILIS, mass separated by HRS and, finally, implanted on the movable tape station at the ISOLDE Decay Sta-

tion (IDS). The measured yield of ^{182}Tl , $1.3 \times 10^5 \frac{\text{ions}}{\mu\text{C}}$, was about an order of magnitude higher than reported in the Yield Database. The detection setup consisted of four standard IDS HPGe clovers, combined with an additional HPGe clover and the SPEDE spectrometer recently developed for ICE measurements [6]. A FWHM-resolution of 7 keV for 300-keV electrons was achieved, allowing the separation of neighboring peaks.

Examples of the γ -ray and electron energy spectra gated on the 1837 keV γ -ray transition in ^{182}Hg are presented in Fig. 1. Prominent peaks at 261 keV and 351 keV are associated with the $4_1^+ \rightarrow 2_1^+$ and $2_1^+ \rightarrow 0_1^+$ transitions, respectively. Preliminary results show an agreement with the known decay scheme, however, the final data analysis is currently ongoing.

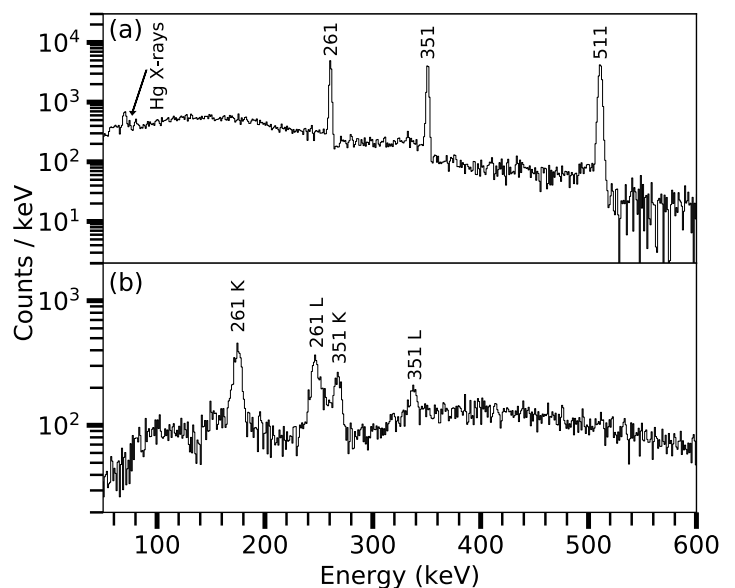


Figure 1: Portions of the background-subtracted (a) γ - and (b) electron energy spectra gated on the 1837 keV transition in ^{182}Hg . The transition energies are given in keV.

References

- [1] K. Heyde, J. L. Wood, *Reviews of Modern Physics* **83**(4), 1467 (2011).
- [2] N. Bree, *et al.*, *Physical Review Letters* **112**(16), 162701 (2014).
- [3] E. Rapisarda, *et al.*, *Journal of Physics G: Nuclear and Particle Physics* **44**(7), 074001 (2017).
- [4] K. Wrzosek-Lipska, *et al.*, 'INTC-P-364' (2012).
- [5] K. Wrzosek-Lipska, L. P. Gaffney, *Journal of Physics G: Nuclear and Particle Physics* **43**(2), 024012 (2016).
- [6] P. Papadakis, *et al.*, *The European Physical Journal A* **54**(3), 42 (2018).

Nuclear structure studies of exotic nuclei: the cases of ^{31}Ar and ^{33}Ar

Results of experiment IS577

Irene Marroquin Alonso for the MAGISOL collaboration

In the IS577 experiment the beta decays of two exotic atomic nuclei were revisited: ^{31}Ar and ^{33}Ar . They are nuclei far from the valley of stability and their respective daughters (^{31}Cl and ^{33}Cl) are de-excited by the emission of protons, which occurs in neutron-deficient nuclei, in this case with $Z > N$ (the IAS is accessible and dominates the decay). This beta-delayed proton emission process is possible due to the low proton separation energy and high Q-value; as a consequence, many decay channels are open and unbound levels are populated in the daughter nucleus [1].

The aim of this work (PhD thesis) was the determination of the resonances of ^{29}P , ^{30}S , ^{31}Cl and ^{33}Cl populated in the decay of ^{31}Ar and ^{33}Ar with the special emphasis in the study of the decay via states near the particle threshold.

Five Double Sided Silicon Strip Detectors (DSSSDs) were used for the proton detection, four of them backed by un-segmented silicon detector (PAD) in telescope configuration. The implantation target, where the ^{31}Ar and ^{33}Ar nuclei decay at rest, was located at the center of the detector set-up. The detection system was placed inside the new implantation/detection chamber, the MAGISOL Si-plugin Chamber, designed within the Madrid-Aarhus-Gothenburg international collaboration, MAGISOL. This novel system had very good energy and angular resolution (25 keV, 3°) as well as

low cut-off energy (150 keV), allowing for the identification of very low energy protons.

The data analysis has provided information such as the half-lives of ^{31}Ar and ^{33}Ar , level energies, spins, parities, width of levels and even density of states. We have determined previously unidentified excited states in ^{33}Cl , thus we can improve the β^+/EC decay scheme of ^{33}Ar [2]. In particular, a total of 13 new transitions of low and medium energy protons in ^{33}Cl have been identified, ranging from 2.5 MeV to 10 MeV. Figure 1 shows the cumulative Gamow-Teller strength deduced in this work versus the excitation energy in ^{33}Cl in comparison with previous results [2].

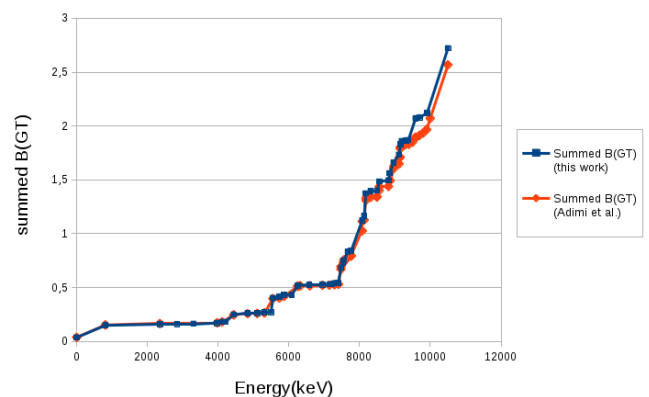


Figure 1: The cumulative Gamow-Teller strength as a function of excitation energy in ^{33}Cl . Our experimental distribution (in blue) is compared to the previous distribution (in orange) obtained in [3]. The figure shows larger values beyond 8 MeV due to the contribution of new weakly fed resonances.

Thanks to different techniques we have also studied

the $\beta 2p$ and $\beta 3p$ channels of ^{31}Ar decay. Some of the results of this study are the determination of three new levels of ^{30}S at high energies above 8 MeV, extending the knowledge of ^{30}S structure and the observation of a large fragmentation in the decay of the IAS of ^{31}Cl to the states of ^{30}S involving all decay channels ($\beta 1p$, $\beta 2p$ and $\beta 3p$). The mechanism of multiple proton emission has also been studied, being mainly sequential. We corroborate previous studies [3, 4].

Furthermore, we have experimentally determined for the first time the partial width of protons and gammas in states of ^{30}S located just above the proton separation energy at energies of 5220(7) keV, 4810(7) keV and 4690(7) keV. The study of the properties of these three states in ^{30}S is very important for nuclear astrophysics, since they have been found to dominate the rate of the $^{29}\text{P}(p,\gamma)^{30}\text{S}$ reaction present in the stellar environments of classical novae. Our experimental values

can be used to calculate the reaction rates (previously, the reaction rates were based on shell model estimated partial widths [5] or experimental limits [6]).

References

- [1] B. Blank, M. Borge, *Prog. Part. Nucl. Phys.* **60**(2), 403 (2008).
- [2] N. Adimi, *et al.*, *Phys. Rev. C* **81**(2), 024311 (2010).
- [3] H. Fynbo, *et al.*, *Nuclear Physics A* **677**(1), 38 (2000).
- [4] G. T. Koldste, *et al.*, *Phys. Rev. C* **89**, 064315 (2014).
- [5] K. Setoodehnia, *et al.*, *Phys. Rev. C* **87**, 065801 (2013).
- [6] G. T. Koldste, *et al.*, *Phys. Rev. C* **87**, 055808 (2013).

RIB applications

Effect of Cd doping on the local structure of vanadium oxides

Results of experiment IS652

Artur W. Carbonari, Anastasia Burimova
IPEN-UFPA collaboration

Vanadium exhibits four common oxidation states +5, +4, +3, and +2, forming V_2O_5 , VO_2 , V_2O_3 and VO oxides, respectively, which enable them to be good candidates for technological applications. Doping with other elements than the native cationic metal can enhance certain properties of these oxides and produce better materials for specific applications or make them suitable for new ones. In the particular case of V_2O_5 , the efforts of doping were mostly aimed at tuning the oxide properties for use as a cathode material in ion batteries, as its layered structure facilitates ion intercalation/extraction [1]. Yet metals are known to interact with vanadium oxoanions resulting in vanadates of different stoichiometries. Usually, synthesis methods do not exclude the possibility of vanadate nucleation. Therefore, a thorough analysis is required to attribute the novel properties to the uniformly solved dopant and not to the contribution of parasitic phases.

In the prevailing number of works the structure of synthesized compounds was monitored by conventional techniques, mostly by X-ray diffraction (XRD). Diffraction peaks distinct from those of orthorhombic V_2O_5 showed up at relatively high dopant (M) concentrations, $x \geq 0.31$ in $M_xV_2O_5$ [2, 3, 4]. However, in [5] the formation of CoV_2O_6 occurred at x as low as 0.05. Tiny discrepancies between XRD patterns of Cu-doped ($x = 0.04$) and bare samples, obtained by the co-precipitation method, can also be observed in [6]. It should be emphasized that post-synthesis procedures often include annealing which, at certain conditions, can lead to partial reduction of V_2O_5 [7]. The size and number of domains where the vanadium oxide was reduced can be very small. With a dominant V_2O_5 phase

it may be challenging to give a correct estimation of the amount of reduced phase even with local techniques like XAFS.

The search for vanadate traces in V_2O_5 with low-level doping can benefit from another local technique – perturbed angular correlation (PAC) spectroscopy. During the ^{111m}Cd beamtime in April of 2018 PAC experiments were carried out by the members of the IPEN-UFPA collaboration in the framework of the IS652 project. For commercial and synthesized samples of V_2O_5 adequate post-implantation annealing procedure was established and the evolution of V_2O_5 hyperfine parameters with temperature was mapped. The second ^{111m}Cd run in October allowed the study of Cd incorporated samples obtained by the co-precipitation method with the Cd:V ratio in the range 0.01 – 0.11 as well as stoichiometric Cd metavanadate. The advantages of Cd to study fundamental effects of doping are the low valence and ease in forming vanadates at the temperatures of interest [8]. Fig. 1 displays the PAC spectra for ^{111m}Cd implanted in V_2O_5 samples doped with different concentrations of Cd and in the CdV_2O_6 compound.

The samples with higher Cd concentration revealed the dominance of sites with $\eta \approx 0.37$ and $\nu_Q \approx 108$ MHz. These parameters were close to those of $Cd(VO_3)_2$ for which a single site with $\eta = 0.4$ and $\nu_Q = 114$ MHz was detected. Intuitively, the Cd site in $Cd(VO_3)_2$ has somewhat modest asymmetry and is expected to have both η and V_{33} lower than those at the V site (see figure 1 a,b). The latter, in turn, appears to have V_{33} smaller and η greater than that of pure V_2O_5 (figure 1 c). Gregoire *et al.* indicated the correlation between the distortion of the first O coordi-

nation shell and the ionic radius of the dopant [9]. Since the ionic radius of Cd is 43% higher than that of V, the obtained values may be attributed to Cd occupying V site of metavanadate. However, we do not exclude the possibility of a V_2O_5 reduction boost due to doping. Another highly distorted site with similar frequency is attributed to dopant or near-dopant site in V_2O_5 . Basing on obtained results, a new series of studies is planned to verify the proposed working hypothesis.

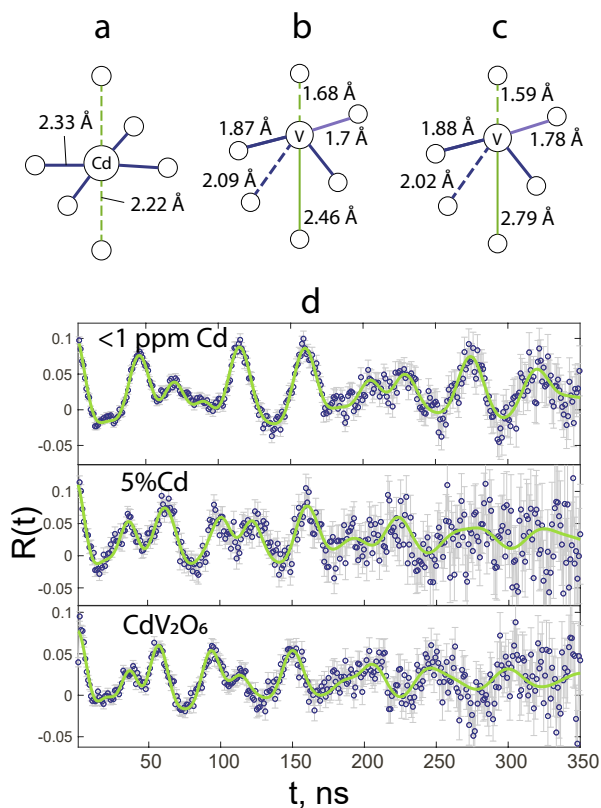


Figure 1: Schematic representation of the first coordination shell of Cd and V ions in CdV_2O_6 (a,b) and of V in V_2O_5 (c); $R(t)$ function for Cd- V_2O_5 systems (d) at 300K

TDPAC: A powerful tool to study TiO_2

Results of experiment IS653

Ian Yap Chang Jie, Juliana Schell, Hans-Christian Hofsäss, Dmitry V. Zybakin, Peter Schaaf
For the University of Göttingen and TU Ilmenau collaboration

Titanium Oxide (TiO_2) is a compound that attracts attention due to its various crystal systems under different temperatures and pressures, along with the po-

References

- [1] F. Coustier, S. Passerini, W. H. Smyrl, *Solid State Ionics* **100**(3–4), 247 (1997).
- [2] C. Xiong, A. E. Aliev, B. Gnade, K. J. B. Jr., *ACS Nano* **2**(2), 293 (2008).
- [3] H. Zeng, *et al.*, *Chem. Mater.* **27**(21), 7331 (2015).
- [4] D. Zhu, H. Liu, L. Lv, Y. D. Yao, W. Z. Yang, *Scripta Materialia* **59**, 642 (2008).
- [5] R. Suresh, *et al.*, *Journal of Alloys and Compounds* **598**, 151 (2014).
- [6] Y. Wei, C.-W. Ryub, K.-B. Kim, *Journal of Alloys and Compounds* **459**, L13 (2008).
- [7] J. Haber, M. Witko, R. Tokarz, *Applied Catalysis A: General* **157**(1–2), 3 (1997).
- [8] M. Bosacka, A. Blonska-Tabero, *J. Therm. Anal. Cal* **93**, 811 (2008).
- [9] G. Grégoire, N. Baffier, A. Kahn-Harari, J.-C. Badot, *J. Mater. Chem.* **8**(9), 2103 (1998).

tential technological application(s) such as its use in thin-film technology as an optical coating for dielectric mirrors, and its usage as a pigment in paint and food

colouring.

TDPAC (Time Differential Perturbed Angular Correlation) is classified as a single atomic probe method in the crystal lattice [1][2]. The material in question is first irradiated, diffused or implanted with the excited probe atoms such as ^{111}In and ^{181}Hf [3], and then thermally annealed to make sure that the original crystal structure remains structurally intact.

We are currently investigating the photocatalytic effect of hydrogenation (via Hydrogen-caused Defects or Hydrogen Doping) on (TiO_2) in its rutile form ($\text{TiO}_2\text{:H}$), at temperatures close to the dissociation of the Titanium-Hydroxide bonds (Ti-OH). Various $\text{TiO}_2\text{:H}$ thin films are prepared in the temperature range between 258°C - 300°C , with 10^{11} ^{111}mCd being implanted as a TDPAC probe. As a control, we have also implanted pure rutile TiO_2 single crystals with the same number of ^{111}mCd .

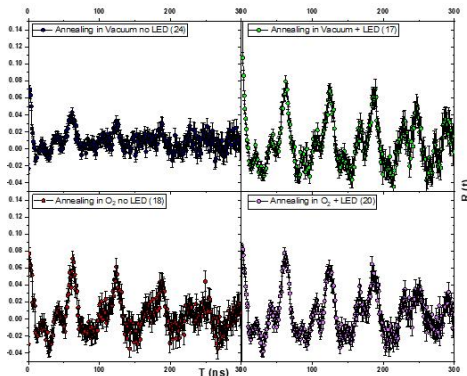


Figure 1: Spectra of the TiO_2 single crystals at room temperature with and without LED illumination, both annealed in Vacuum or in Air. [4]

Preliminary visual analysis of the spectra suggests that under the effects of the laser illumination of a 365 nm LED diode on both single crystals, there is a significant change in the frequency distribution and the gamma anisotropy for the samples annealed under an oxygen-deficient atmosphere.

The difference in EFG of the probe atom due to the oxygen vacancies located close to the probe is observable under the timescale of the TDPAC measurements.

In addition, further experiments regarding $\text{TiO}_2\text{:H}$ films measured under different atmospheric conditions were performed, to verify how this scenario is independent of the induced defects.

With this experiment in mind, we also hope to complement the gamma-gamma method with the electron-gamma technique. It could be of great advantage for studying materials such as TiO_2 by extending the number of available probe nuclei. It could provide additional local information about the temperature dependent defect or electronic defect local configuration in the neighbourhood of the TDPAC probe.

References

- [1] J. Schell, P. Schaaf, and D. C. Lupascu, "Perturbed angular correlations at isolde: A 40 years young technique," *AIP Advances*, vol. 7, p. 105017, 10 2017.
- [2] G. Schatz and A. Weidinger, *Nuclear Condensed Matter Physics: Nuclear Methods and Applications*. Wiley, 1992.
- [3] J. Schell, D. C. Lupascu, A. W. Carbonari, R. Domingues Mansano, I. Souza Ribeiro Junior, T. T. Dang, I. Anusca, H. Trivedi, K. Johnston, and R. Vianden, "Ion implantation in titanium dioxide thin films studied by perturbed angular correlations," *Journal of Applied Physics*, vol. 121, no. 14, p. 145302, 2017.
- [4] D. Zyabkin, J. Schell, D. C. Lupascu, H. P. Gunnlaugsson, H. Masenda, R. Mantovan, K.-B.-Ram, S. Olafsson, H. P. Gislason, B. C. Qi, P. Rkastev, J. G. M. Correia, U. Vetter, and P. Schaaf, "Hyperfine interactions in hydrogenated titanium oxide thin films and powders for photocatalytic reactions, experiment is653, proposal to the isolde and neutron time-of-flight committee," tech. rep., ISOLDE-CERN, 2018.

Technical changes and updates on the On-line Diffusion Chamber (ODC)

Results of experiment IS627

Daniel Gaertner for the SSP-collaboration

Inspired by an ion-beam sputtering device for diffusion studies built by Wenwer et. al. [1] the On-line Diffusion Chamber (ODC) was built for diffusion studies in which the single steps - named by implantation of the isotope into the sample, diffusion annealing, sectioning using the ion-beam sputtering technique, counting the activity of each section using a gamma-detector - can be performed in-situ. The original setup contained an *Agilent ATP 250* turbo-pump, a *Gero* vacuum furnace including a water flow control and a *Deditec* shutter, a *Veeco MPS-3000 FC* ion-beam sputtering device including a *Schaefer* gas-flow control, a ceramic sample-holder with integrated axis translation, rotation and a thermocouple, a combination of a Faraday-Cup and an aperture, a spool of film and a *Canberra* NaI-detector with a 16K multi-channel analyzer. In order to decrease the processing time for the experiments the following changes and updates of the ODC were performed: The *Gero* vacuum furnace and all related parts were removed and the position of the turbo-pump was changed, therefore the chamber volume was decreased and the necessary high-vacuum of $< 10^{-6}$ mbar could be reached faster. A stainless steel sample holder with a heating plate on top ($T_{\max} \approx 720^\circ\text{C}$ - controlled by an *Omega Micromega CN77000* PID-control) replaced the former holder. The sample will be fixed on a tungsten-copper alloy socket with an integrated thermocouple. Due to the self-heating functionality of the sample holder, the axis translation was removed. All changes were included in the *LabView* program concerning to the ODC. Figure 1 represents the process of an on-line diffusion experiment schematically: After fixing the sample on the tungsten-copper socket and inserting it into the ODC, the chamber will be pumped to high-vacuum. The sample holder will be

heated up to the intended diffusion annealing temperature and rotated by 90° in order that the sample surface faces the implantation beam. The current of the implantation beam can be checked using the Faraday-Cup, which is initially positioned in front of the sample. While the aperture is moved into the beam line, the implantation process and diffusion annealing starts. After implanting the isotope the sample holder will be rotated back to the sectioning position and the sectioning process starts. Atoms of pure Ar-gas with a flow of 12 – 15 SCCM (Standard Cubic-Centimeter per Minute) will be ionized. The Ar^+ ions will move towards a pair of isolated and parallel aligned grids and will be accelerated towards the sample surface normal forming an angle of 60° . Depending on the adjustable duration of the beam, the thickness of the section can be set manually. Each section will be intercepted by a film and their activity will be counted and analyzed by energy discrimination with the NaI-detector. With the present setup, diffusion profiles with a bulk-diffusion length of maximum $2\ \mu\text{m}$ can be produced and measured.

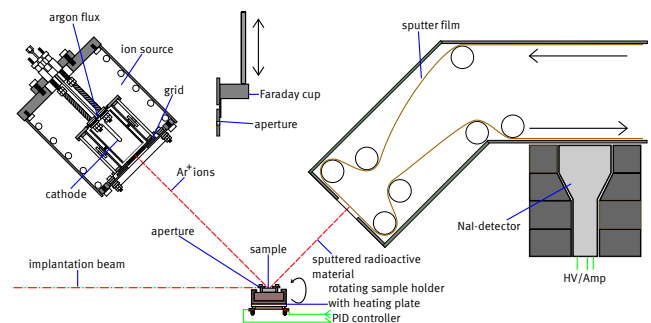


Figure 1: Schematical setup of the new On-line Diffusion Chamber.

References

- [1] F. Wenwer, et al., *Measurement Science and Technology* **7**, 632 (1996).

Beamline upgrades and first biological studies

Results of experiment IS645

Jared Croese for the BetaDrop NMR Team

Nuclear Magnetic Resonance (NMR) is a versatile and widely used spectroscopic technique. However it suffers from an inherent insensitivity due to the very small amount of thermal polarization at room temperature. This is especially problematic when studying low abundant quadrupolar nuclei in living systems.

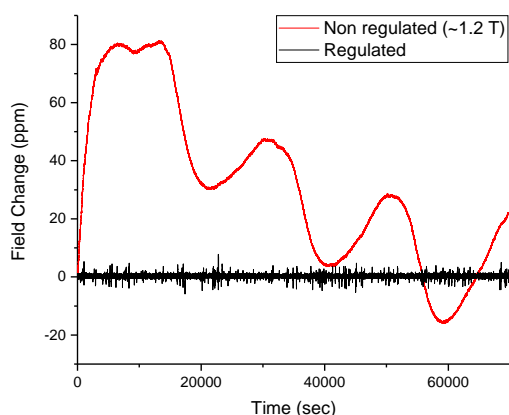


Figure 1: Magnetic field oscillations in parts per million (ppm) over time before and after the implementation of a stabilization mechanism. The red line indicates the non-regulated magnetic field and the black line the regulated magnetic field

An example of such a system is a Guanine Quadruplex (GQ). GQs are special four-stranded DNA conformations that can be formed in guanine-rich areas of the DNA in the presence of alkali metal ions. Among other places GQs are found in the telomeric regions of the DNA and they are considered to be promising new molecular anti-cancer targets. They are detectable in human cells and are strongly suspected to be involved in a number of biological processes at the DNA and RNA levels. The low concentrations of, for example, Na ions needed to form these structures mean that a more sensitive NMR technique is needed to study them.

The goal of IS645 is to apply the ultra sensitive β -NMR technique to liquid bio-molecular samples for biochemical studies[1]. The interaction of GQ's with Na⁺ will serve as the first demonstration of this application.

Last year we reported a major step towards achieving the goal of IS645 with our first well resolved Na β -NMR signal from an ionic liquid[2]. During 2018 the beamline saw major upgrades and we successfully measured a signal from a biological sample.

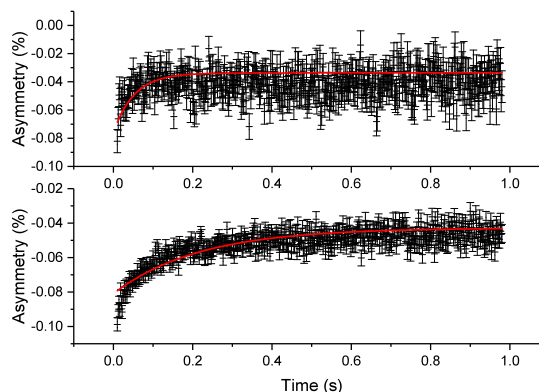


Figure 2: NMR Relaxation curves of an empty mica substrate (top) and a mica substrate covered in DNA (bottom). The y-axis shows the beta decay asymmetry and the x-axis the time in seconds. Both curves have been fitted with an exponential decay giving a 50 ms relaxation time for the empty mica substrate and a 500 ms relaxation time for the one covered with DNA.

The first upgrade was the implementation of a new type of a voltage scanner and a new charge exchange cell hosted in a light all-aluminum vacuum chamber[3]. This allowed unwanted beam steering effects to be solved and made it a more user-friendly device. The second was a new sample handling system which reduced the time requirements of changing samples by 60 fold. The next was a home-built vacuum-compatible NMR magnetometer allowing the monitoring of the magnetic field a few mm from the sample site. This enabled the development of a magnetic field stabilization system that improved the temporal stability by two orders of magnitude as shown in Fig. 1. The last upgrade was the doubling of the magnetic field strength and the improvement of the magnetic field homogeneity at the measurement site by replacing the electromagnet. As

part of this upgrade a new measurement chamber and a set of PCB shimming coil plates were designed and connected to the beamline.

Due to problems with magnetic field instability during a beamtime that took place in the summer we focused on making NMR relaxometry measurements during which we measured a T1 relaxation time of 50 ms for an empty mica substrate and of 500 ms for DNA on this same substrate as shown in Fig. 2. The interpretation of this difference is part of an active discussion with our collaborators from Ljubljana and Poznan.

During October's beamtime, after applying the B_0 regulation and increasing its homogeneity, both chemical shifts (resonances) and T1 relaxation times were measured from samples containing Guanines (2Na 5'-GMPs) and Crown-ethers (15C5) dissolved in Ionic Liq-

uids (ILs) BMIM-HCOO or EMIM-DCA, or a deep eutectic solvent known as 4:1 Glycoline. The data are being analyzed, while complementary conventional NMR and T1 relaxation measurements using stable ^{23}Na and ^1H nuclei are being performed at Leipzig and Poznan Universities for a better description and understanding of these systems .

References

- [1] M. Kowalska, *et al.*, *CERN-INTC-2017-071/INTC-P-521* (2017).
- [2] M. Kowalska, *et al.*, *CERN-INTC-2018-019/INTC-P-521-ADD-1* (2018).
- [3] W. Gins, *et al.*, *Nucl. Instrum. Methods Phys. Res. A* **925**, 24 (2019).

^{11}Be lattice location in GaN as function of temperature and doping type

Results of experiment IS634

Ulrich Wahl for the EC-SLI collaboration

The interest in Be as an impurity in GaN stems from the challenge to understand why it is technologically feasible to dope this wide band gap semiconductor p -type with Mg, while this was not successful for Be. While theory has actually predicted acceptor levels for Be that are shallower than for Mg [1, 2, 3], it was also argued that Be would not be a suitable acceptor because its amphoteric nature (i.e. its tendency to occupy both substitutional Ga and interstitial sites) should be considerably more pronounced than for Mg and hence lead to complete self-compensation [2]. The amphoteric character of Mg was recently proven using our Emission Channeling with Short-Lived Isotopes (EC-SLI) technique [4]. In a similar way we have now determined the lattice location of ^{11}Be ($t_{1/2} = 13.8$ s) in several doping types of GaN as a function of implantation temperature. We found that interstitial ^{11}Be fractions were much higher than in the case of ^{27}Mg ; for RT implanta-

tion interstitial Be was in fact dominating except for in n -type GaN. This confirms that indeed self-compensation should be considerably more pronounced for Be than for Mg. While both interstitial Mg_i and Be_i are located in the wide open interstitial region of the GaN lattice parallel to the c -axis, their exact positions differ considerably by 1.3\AA (Fig. 1). The Be_i location determined by EC-SLI coincides within 0.06\AA with theoretical predictions [2, 3, 5]. There was less influence from implantation damage for ^{11}Be than for ^{27}Mg ; hence $^{11}\text{Be}_i$ was sustained for longer implantation times and is therefore a more sensitive Fermi-level probe than $^{27}\text{Mg}_i$. Major site changes of interstitial Be_i to substitutional Be_{Ga} started around 400°C in undoped GaN and n -GaN:Si, thus roughly at the same temperature as for ^{27}Mg . This is a bit of a surprise since the interstitial Be thus seems to show a similar migration energy as Mg, somewhat in contrast to theoretical predictions [2, 5]. While in p -

GaN:Mg the site change of ^{11}Be also started at 400°C , Be did not totally disappear from interstitial sites but was only reduced to $\sim 15\%$. There was then a clear further stage at 750°C , and so only at 800°C was Be_i completely converted to substitutional. A possible explanation seems to be the formation of $\text{Be}_i\text{-Mg}_{\text{Ga}}$ pairs that slow down Be_i diffusion until these pairs are broken up.

References

- [1] F. Bernardini, V. Fiorentini, A. Bosin, *Appl. Phys. Lett.* **70**, 2990 (1997).
- [2] C. G. de Walle, S. Limpijumnong, J. Neugebauer, *Phys. Rev. B* **63**, 245205 (2001).
- [3] C. D. Latham, *et al.*, *Phys. Rev. B* **67** (2003).
- [4] U. Wahl, *et al.*, *Phys. Rev. Lett.* **118** (2017).
- [5] G. Miceli, A. Pasquarello, *phys. stat. sol. RRL* **11**, 1700081 (2017).

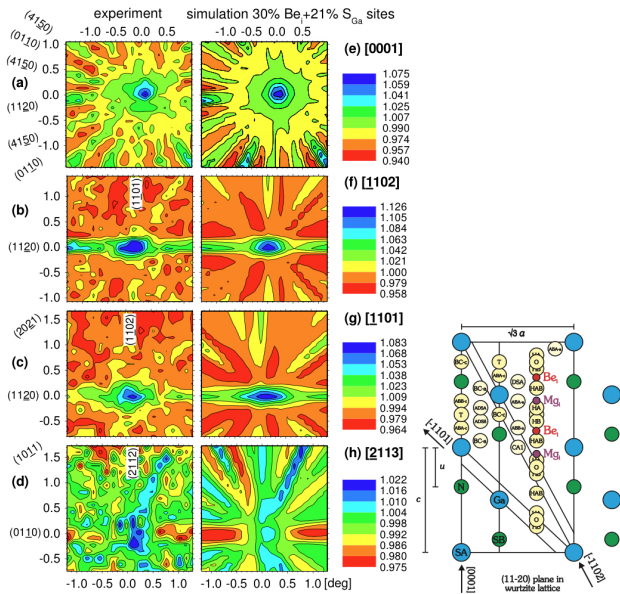


Figure 1: (a)-(d) are experimental β^- emission patterns from ^{11}Be in undoped GaN in the vicinity of $\langle 0001 \rangle$, $\langle -1102 \rangle$, $\langle -1101 \rangle$, and $\langle -2113 \rangle$ axes obtained at 20°C ; (e)-(h) are best fits of simulated patterns, corresponding to 30% on interstitial Be_i sites and 21% on substitutional $\text{Ga}(\text{S}_{\text{Ga}})$. Note that fractions are not yet corrected for background. Right: (11-20) plane in the GaN wurtzite lattice, showing the substitutional S_{Ga} (SA) and S_{N} (SB) positions and the major interstitial sites. The positions of interstitial Be_i and Mg_i from EC-SLI experiments are indicated by the red and purple circles.

Studies with post-accelerated beams

A new triple foil plunger for lifetime measurements with MINIBALL/HIE-ISOLDE

*Liam Barber, Michael Giles, Dave Cullen, Andy Smith,
Andy McFarlane
The University of Manchester*

The differential decay curve method (DDCM) is a well established technique for making lifetime measurements of excited nuclear states with a two foil plunger [1]. The plunger allows for the excited nuclei to travel at two different velocities and so γ -rays are detected with one of two Doppler shifts. This provides information on the fraction of the excited recoils that decay between the two foils separated by a distance x . As DDCM relies on knowledge of the differential of this decay curve, γ -ray measurements must be made at several, typically 6 to 10, values of x .

A triple foil plunger has been designed at The University of Manchester which was commissioned in early 2018 at the University of Jyväskylä [2]. A target foil and two degrader foils are separated by distances x and $x + \Delta x$, respectively. The presence of a third foil divides γ -rays into three Doppler-shifted energies, at velocities $v_{1,2,3}$. This allows for both the decay curve and its differential to be measured at a single plunger distance by measuring the decay curve at a distance x and $x + \Delta x$, by approximating the differential as $(I(x+\Delta x) - I(x))/\Delta x$ providing $\Delta x/v_2 \ll \tau$ [1].

It was shown during the commissioning that the use of a triple foil plunger over a conventional two foil plunger results in a beamtime reduction of ~ 2.5 for particle-tagged γ events and ~ 3.5 for untagged γ events [2]. This means that lifetimes can be measured in channels that previously would have been infeasible due to low production cross sections.

A second triple foil plunger is currently under construction optimised for use with MINIBALL and HIE-

ISOLDE after LS2. The following adaptations have been made with the new design:

- Smaller central chamber that contains the three foils and two motors to allow for the plunger to be placed within the MINIBALL chamber.
- Downstream of foils adapted to allow for DSSD and electronics for kinematic reconstruction of COULEX events.
- Foil separations down to $\sim 10 \mu m$, corresponding to lifetime measurements from in the picosecond-range.

This device will allow for low cross section COULEX lifetime measurements to be made. The use of a plunger to make lifetime measurements has advantages over relying on COULEX cross sections to determine transition rates. The need for an absolute cross section and knowledge of the magnitude and sign of several matrix elements are removed. Additionally, however, the use of a triple foil plunger results in a factor of ~ 3 beamtime improvement compared to a conventional plunger. This device will be ready for use after LS2.

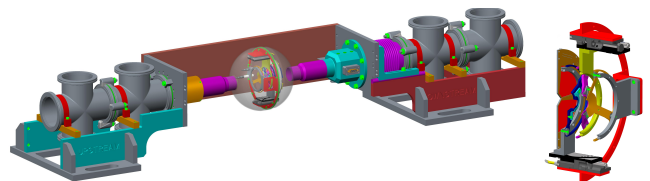


Figure 1: A CAD drawing of the triple foil plunger, adapted to fit into MINIBALL and incorporate a backward-angled DSSD.

References

[1] A. Dewald, O. Moller, P. Petkov, *Progress in Particle and Nuclear Physics* **67**(3), 786 (2012).

[2] M. M. Giles, et al., *Nuclear Instruments and Methods in Physics (Accepted, to be published)* (2019).

Coulomb Excitation of Pear-Shaped Nuclei

Results of experiment IS552

Peter Butler, Liam Gaffney, Pietro Spagnoletti for the IS552 collaboration

We have carried out measurements, using Miniball, of the γ -ray de-excitation of $^{222,228}\text{Ra}$ and $^{222,224,226}\text{Rn}$ nuclei Coulomb-excited by bombarding ^{60}Ni and ^{120}Sn targets. The beams of radioactive ions, having energies of between 4.25 and 5.08 MeV.A, were provided by HIE-ISOLDE. The purpose of these measurements is to determine the intrinsic quadrupole and octupole moments in these nuclei and look for other cases of permanent octupole deformation to those of $^{224,226}\text{Ra}$ already reported [1, 2].

One aim of this experiment is to determine the level schemes of $^{224,226}\text{Rn}$ in order to characterise these isotopes as octupole vibrational or octupole deformed. Figure 1 shows the spectra of γ -ray in coincidence with scattered $^{222,224,226}\text{Rn}$ beam and ^{120}Sn recoils.

larity, and to depopulate the odd-spin negative-parity members of the octupole band. In order to determine which states are connected by these transitions, pairs of coincident γ -rays were examined. Typical spectra obtained this way are shown in Fig. 2.

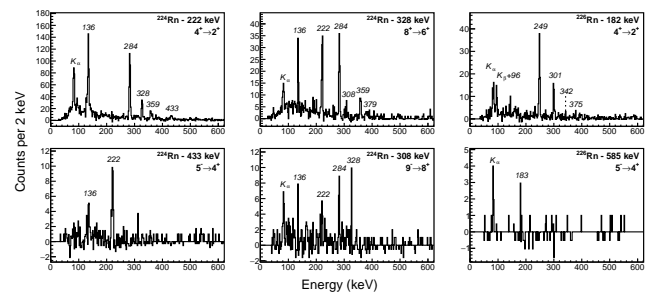


Figure 2: Representative background-subtracted γ -ray spectra in time-coincidence with different gating transitions. Here the observed peaks are labelled by the energy (in keV) of the transition.

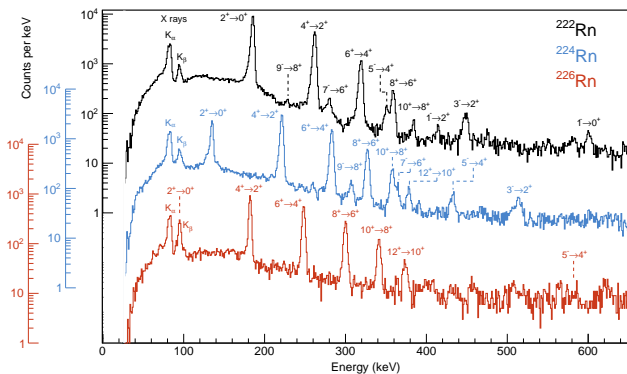


Figure 1: Spectra of γ -rays following the bombardment of ^{120}Sn targets by ^{222}Rn (black), ^{224}Rn (blue), and ^{226}Rn (red). The γ -rays are corrected for Doppler shift assuming that they are emitted from the scattered projectile.

The E2 γ -ray transitions within the ground-state positive-parity band can be clearly identified. The other relatively intense γ -rays observed in these spectra with energies < 600 keV are assumed to have E1 multipo-

Level schemes for the virgin nuclei $^{224,226}\text{Rn}$ were constructed from the coincidence spectra. From these level schemes it was possible to explore the character of the octupole bands by examining the difference in aligned angular momentum, $\Delta i_x = i_x^- - i_x^+$, at the same rotational frequency ω , as a function of ω . The preliminary results of this analysis suggests that radon even-even nuclei in this mass region are all octupole vibrational, which has implications for EDM searches in radon atoms.

References

- [1] G. L. P. et al., *Nature* **497**, 199 (2013).
 [2] W. H. J. et al., *Nuclear Physics A* **556**, 261 (1993).

A new frontier: direct reactions on nuclei below ^{208}Pb with $N = 126$

Results of experiment IS631

B. P. Kay for the ISS collaboration

The region south and east of ^{208}Pb , as shown in Fig. 1(a), is one of the last remaining unexplored territories on the chart of nuclides. Essentially nothing is known of single-particle excitations outside of the closed shell $N = 126$. This is in part due to the difficulties of producing intense radioactive beams of these isotopes at energies above the Coulomb barrier and the lack of availability of charged-particle spectrometers with excellent Q -value resolution and solid angle coverage. At ISOLDE, both of these things are now available via the high-intensity and energy upgrade of the linac and the new ISOLDE Solenoidal Spectrometer (ISS).

To start exploration of this region, the ISS collaboration carried out a measurement of the $^{206}\text{Hg}(d,p)^{207}\text{Hg}$ reaction in inverse kinematics. This was motivated by recent studies of weak-binding effects in nuclei [1]. The ^{206}Hg beam was accelerated to 7.4 MeV per nucleon (1.52 GeV) and steered to the ISS. The Si detector and data-acquisition system were from the HELIOS spectrometer [2] at Argonne National Laboratory, the instrument that inspired the development of the ISS.

The beam was remarkable, having an intensity of $3\text{--}8 \times 10^5$ particles per second, and a purity of greater than 98%. This was achieved using VADLIS to selectively ionize the mercury atoms and suppress the lead target material at the same mass [3].

Excited states in ^{207}Hg were seen for the first time, with a Q -value resolution of ~ 130 keV FWHM [Fig. 1(b)]. These have been determined to be major components of the neutron $1g_{9/2}$, $2d_{5/2}$, $3s_{1/2}$, $2d_{3/2}$, and $1g_{7/2}$ strengths from the proton angular distributions [e.g., Fig. 1(c)]. While the pattern of the centroids is similar to ^{209}Pb , there is substantial fragmentation of the $2d_{5/2}$ strength. The interpretation of the data is ongoing.

This is the heaviest beam used for such studies and

marks the start of an exciting program of reaction studies with heavy beams at ISOLDE using the ISS.

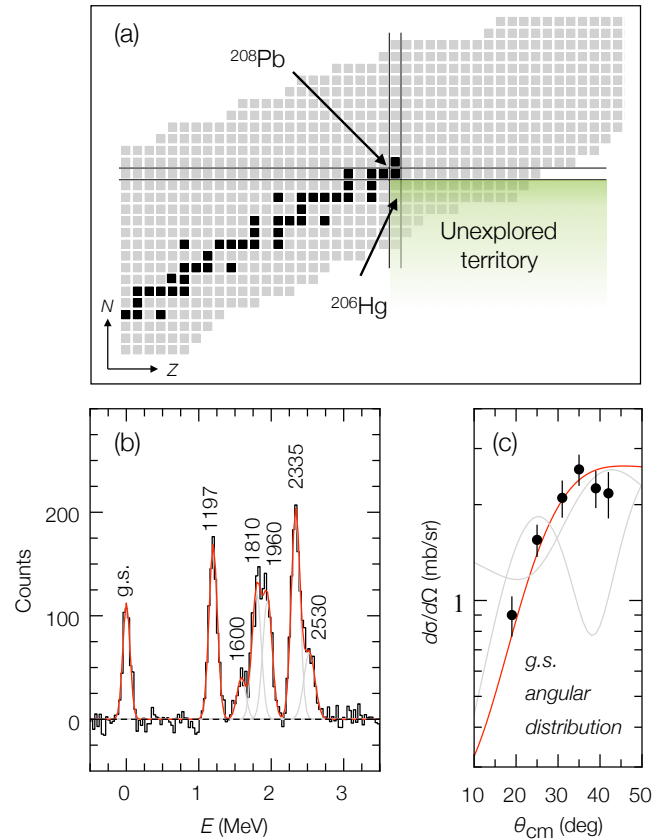


Figure 1: (a) The unexplored territory south east of doubly magic ^{208}Pb on the nuclear chart. (b) The outgoing proton spectrum from the $^2\text{H}(^{206}\text{Hg},p)$ reaction as measured with ISOLDE Solenoidal Spectrometer, providing the first observation of the structure of ^{207}Hg , and (c) the ground-state angular distribution confirming it to be a $1g_{9/2}$ configuration.

References

- [1] C. R. Hoffman, B. P. Kay, J. P. Schiffer, *Phys. Rev. C* **89**, 061305 (2014).
- [2] J. C. Lighthall, *et al.*, *Nucl. Instrum. Methods Phys. Res. A* **622**, 97 (2010).
- [3] T. D. Goodacre, *et al.*, *Nucl. Instrum. Methods Phys. Res. B* **376**, 39 (2016).

First measurements using the ISOLDE Solenoidal Spectrometer $^{28}\text{Mg}(d,p)^{29}\text{Mg}$

Results of experiment IS621

David Sharp for the ISS collaboration

In September 2018 the first physics measurement with the ISOLDE Solenoidal Spectrometer (ISS) took place. The $^{28}\text{Mg}(d,p)^{29}\text{Mg}$ reaction was performed in inverse kinematics with a beam of ^{28}Mg at an incident beam energy of 9.473 MeV/u and intensity of 10^6 pps. The delivery of this beam at this energy represents a milestone for HIE-ISOLDE being the highest energy per nucleon radioactive beam delivered to an experiment.

The ISS is yet to be fully commissioned, with its own silicon array still under construction at the University of Liverpool and Daresbury Laboratory. Thanks to collaborators from the HELIOS experiment at Argonne National Laboratory, USA, an early implementation phase of the project allowed physics measurements to run before CERN's LS2. The position-sensitive silicon array and the associated digital data acquisition system used in HELIOS [1] was shipped to ISOLDE for this purpose.

The aim of this measurement was to probe the evolution of single-particle behaviour both towards the island of inversion, where deformed ground states and low-lying excitations are prevalent, and along the $N = 17$ isotones [2], probing the emergence of the $N = 16$ shell closure in ^{24}O . Of particular interest is the behaviour of the negative-parity orbitals that drive the onset of the observed phenomena in this region. States in ^{29}Mg were populated via the (d,p) reaction, with the emitted protons detected in a position-sensitive array upstream of a CD_2 target, after they have executed a helical orbit in the field of the solenoid. Downstream of the target was a silicon dE-E recoil detector to allow identification of the magnesium recoils, and provide a timing reference to identify protons from their cyclotron period. Figure 1 shows the energy and position of the protons from the target measured in the array, with the resulting excitation energy spectrum for ^{29}Mg also shown, where the observed resolution is ~ 120 keV.

The analysis for this work is still ongoing but will provide a robust determination of the single-particle centroids thanks to identification of significant fragments of strength above the neutron separation energy.

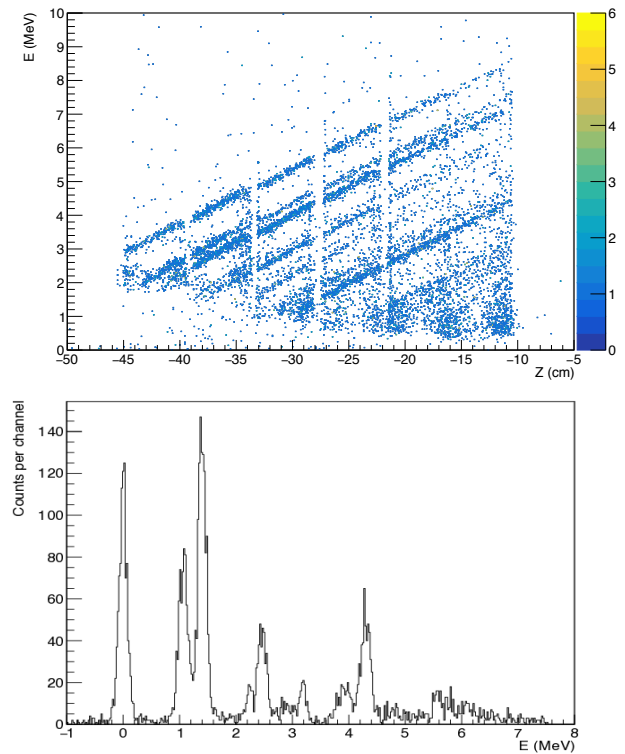


Figure 1: (Top) Plot of measured proton energy against the position from the target that the proton is incident on the silicon array. (Bottom) Excitation energy spectrum for states in ^{29}Mg .

References

- [1] J. Lighthall, *et al.*, *Nuclear Instruments and Methods in Physics Research Section A: Accelerators, Spectrometers, Detectors and Associated Equipment* **622**(1), 97 (2010).
- [2] D. K. Sharp, *et al.*, 'Single-particle behaviour towards the "island of inversion" - $^{28,30}\text{Mg}(d,p)^{29,31}\text{Mg}$ in inverse kinematics', Tech. Rep. CERN-INTC-2016-030. INTC-P-470, CERN, Geneva (2016).

Halo effects in the low-energy scattering of ^{15}C with heavy targets.

Results of experiment IS619

*J.D. Ovejas, I. Martel, O. Tengblad, M.J.G. Borge,
N. Keeley for the IS619 collaboration*

High-energy scattering studies (*i.e.* ~ 100 MeV/u), have previously suggested a halo structure for the weakly bound isotope ^{15}C [1]. The collision process at these energies is sensitive to the single-particle structure of the ground-state wave function and the presence of a neutron halo would produce, as has been observed, a narrow transverse-momentum distribution for one-neutron breakup and a large value of the total interaction cross section, in comparison with its neighbouring isotopes $^{14,16}\text{C}$. However, at low collision energies, around the Coulomb barrier (*i.e.* ~ 5 MeV/u), the dynamics of the system would be dominated by collective degrees of freedom, and it would be characterised by the coupling between the elastic, transfer and breakup channels, as well as the effects of the continuum. The halo structure should therefore manifest in collisions with heavy targets by a strong absorption pattern in the differential elastic cross section and the suppression of the nuclear rainbow as shown in Fig. 1 following the calculations of [2].

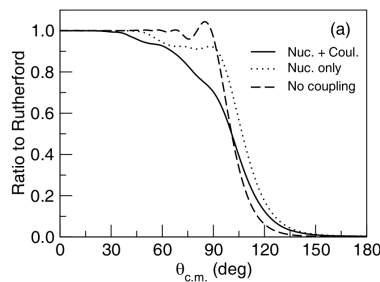


Figure 1: CDCC (Continuum Discretized Coupled Channels) calculations for ^{15}C on ^{208}Pb at 65 MeV. The dashed curve shows the optical model (no coupling), the dotted line includes the nuclear coupling, and the solid one the breakup coupling.

Aiming to probe this debated structure, the first dynamic study of ^{15}C at energies around the Coulomb barrier was carried out in August 2017 at SEC (Scattering Experiment Chamber), in the third beamline of HIE-ISOLDE. For this purpose, a $^{15}\text{C}^{5+}$ beam was produced from a CaO primary target, post-accelerated up

to 4.37 MeV/u and made to impinge on ^{208}Pb targets (2.1 and 1.2 mg/cm² thick). $^{15}\text{N}^{5+}$ and $^{12}\text{C}^{4+}$ (with the same $A/q=3$) were also present in the beam before the 75 $\mu\text{g}/\text{cm}^2$ carbon foil. After the stripping process the nitrogen presence resulted in $^{15}\text{C}/^{15}\text{N} \sim 0.03$, while ^{12}C was removed. The ^{15}C beam intensity was estimated leading to an averaged yield of about 10^3 pps. The measurement of the ions following the reaction was performed with the GLORIA detector array [3]. It consists of 6 silicon telescopes made up of two DSSDs; a 40 μm thick ΔE in the front and a second 1 mm E in the back. The detectors surrounded the reaction target, covering scattering angles from 15° to 165° in a laboratory system with total geometric efficiency of 25%. Analysis is ongoing, for which, in order to determine the differential elastic cross-section, the pixels are grouped within an averaged scattering angle $\theta \pm \Delta\theta$. Plotting the two-dimensional ΔE -E figures for each group of pixels, where the same physics is expected, different ions and reaction channels can be separated and properly integrated, as depicted in Fig. 2. The differential elastic cross-section of ^{15}C up to 110° will be determined.

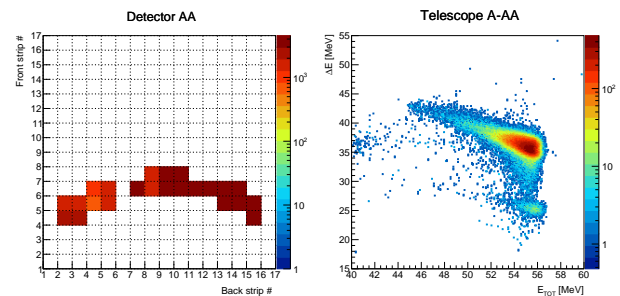


Figure 2: On the left hand side, a set of pixels covering the angular sector $34^\circ \pm 2^\circ$. On the right hand side, the corresponding two-dimensional plot. The elastic events can be clearly distinguished: ^{15}N spot in the upper part and ^{15}C in the lower one.

References

[1] A. Ozawa, *Nucl. Phys. A* **738**(3844) (2004).

[2] N. Keeley, *Eur. Phys. J. A* **50**(145) (2014).

(2014).

[3] G. Marquez-Duran, *Nucl. Inst. Meth. A* **755**(69)

Shadow readout at the SEC

Michael Munch, Jesper H. Jensen, Håkan T. Johansson
MAGISOL

The scattering experiment chamber (SEC) located at XT03 is designed as a versatile chamber allowing it to be used by a large variety of experiments which typically employ an array of segmented silicon detectors with 200–400 channels. The large number of channels, together with the pulsed HIE-ISOLDE beam, places tough requirements on the data acquisition system (DAQ).

The DAQ at the SEC is based on analog signal processing, with modular VME ADCs and TDCs writing data in list mode. Depending on the modules used, an event can be digitized in 1 to 7 μs with an additional 1 to 4 μs gate time. However, with the VME processors available, the readout time would typically be much larger than this. This becomes a problem when data is transferred during deadtime.

To circumvent this issue we have developed a new readout scheme called *shadow readout* [1]. The main idea is to continuously transfer data from the modules to the processor, outside deadtime. With this change, deadtime is almost completely avoided, leaving only the busy times of digitization. An example of the achieved performance with six CAEN v785 ADCs, can be seen in Fig. 1, which shows the livetime, i.e. the fraction of accepted events, as a function of the number of triggers accepted. For this specific example, the deadtime at 25 kHz is reduced from roughly 60% to 15%. The blue dotted line shows the performance of the old multi-event readout scheme, while the red solid line shows the performance of the improved readout scheme. This line corresponds to a deadtime of 10 μs per event,

which is the conversion and gate time for the ADC. In comparison the old mode gives an effective deadtime per event of 30 μs . The sharp drop at 54 kHz corresponds to the saturation of the VME processor. With an improved VME processor, the limit could be pushed to higher rates, as indicated by the dashed red line.

With this improved readout scheme, the DAQ should be able to handle the data from even larger silicon arrays at the SEC. The interested reader can consult Ref. [1] for more details.

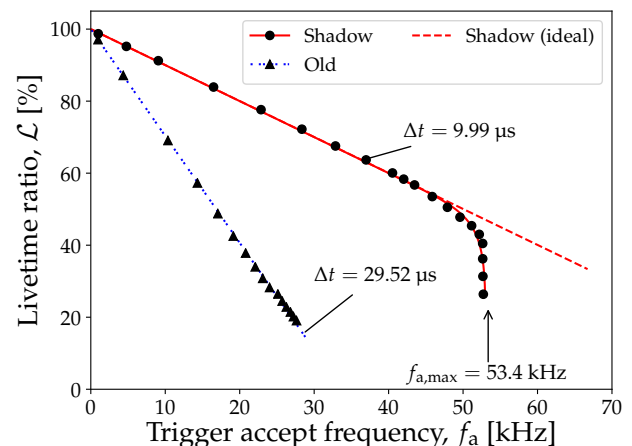


Figure 1: Measured performance of the shadow readout for a system with six CAEN v785, shown with black dots and a solid red line. The performance of the old readout scheme is shown as dotted blue. With an improved VME processor, it would be possible to achieve even better performance, shown as dashed red.

References

- [1] M. Munch, J. H. Jensen, B. Loher, H. Tornqvist, H. T. Johansson, *IEEE Transactions on Nuclear Science* pp. 575 – 584 (2019).

Beta decay of ^{11}Be

Results of experiment IS629

Chiara Mazzocchi for the IS629 collaboration

β -delayed proton (βp) emission is a phenomenon that happens typically in very proton-rich nuclei. Interestingly, in a few, light neutron-rich nuclei, the energy window for this process is also open. One such case is ^{11}Be , for which several channels for β -delayed particle emission are open, including the βp ($Q_{\beta p} \sim 280$ keV) and the β -delayed α ($\beta\alpha$) branches. Theoretical predictions for the βp branching ratio ($b_{\beta p}$) give very low values, of the order of 10^{-8} [1]. Indirect observations based on accelerator mass spectrometry (AMS) [2, 3] resulted in a $b_{\beta p}$ value two orders of magnitude larger than predicted. Such a surprisingly large value can be explained (within the current models) only if the decay proceeds through a new single-particle resonance in ^{11}B strongly fed by β decay [3]. The B(GT) value for this transition could be as high as 3, which corresponds to the free-neutron decay, as it would be when the halo neutron decays into a single-proton state. Direct measurement of the $b_{\beta p}$ and energy spectrum is therefore important for estimating the B(GT) at high excitation energies and for testing models that predict a direct relation between βp and halo structure. Furthermore, recently a new hypothesis which may explain the results of the AMS experiment, appeared. According to it, the neutron may have another decay channel in which unknown particles are produced in the final state [4, 5].

The experiment was performed between August and September 2018 using the Warsaw optical-readout Time Projection Chamber (OTPC)[6] with a new data-acquisition mode to handle the particularly challenging experimental requirements, like, e.g., the long half-life of ^{11}Be (13.8 s) [7]. The OTPC records tracks of charged particles (ions, protons, α s), but is not sensitive to β electrons. This characteristic greatly suppresses the background, rendering the measurement of low-energy charged-particles possible. The full 3D

reconstruction of the tracks combines the 2D image of the decay taken by a CCD camera and the drift-time profile measured by a photomultiplier.

The ^{11}Be ions were produced by the 1 GeV proton beam impinging on a UC_x target, ionised in the RILIS ion source, separated by the GPS, post-accelerated by HIE-ISOLDE and implanted into the active volume of the OTPC detector, which was installed downstream of the scattering chamber at the XT03 beam-line. An example image collected by the CCD camera of the OTPC, showing three $\beta\alpha$ particles from the decay of ^{11}Be , is given in Fig. 1.

Over 5 days of beam-time about 50×10^6 ^{11}Be ions were implanted into the active volume of the OTPC detector. About 1.5×10^6 $\beta\alpha$ particles were detected in the $\sim 1.4 \times 10^6$ images recorded. The statistics collected allow the search for βp emission from ^{11}Be with a sensitivity of $\sim 10^{-7}$. Analysis of the data is in progress.

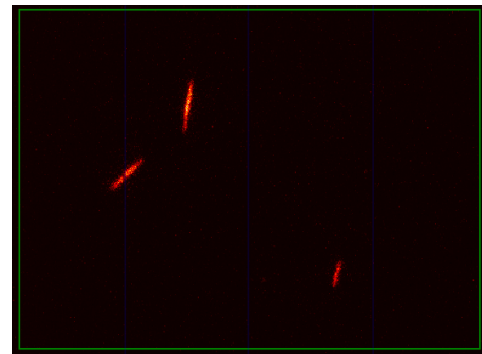


Figure 1: Example CCD image from one of the events collected. Three $\beta\alpha$ particles are clearly visible.

References

- [1] M. B. et al., *J. Phys. G* **40**, 035109 (2013).
- [2] K. Riisager, *Nucl. Phys. A* **925**, 112 (2014).
- [3] K. R. et al., *Phys. Lett.* **B732**, 305 (2014).
- [4] B. Fornal, B. Grinstein, *Phys. Rev. Lett.* **120**, 191801 (2018).

- [5] M. Pfützner, K. Riisager, *Phys. Rev. C* **97**, 042501(R) (2018).
 [6] A. C. et al., *Eur. Phys. J. A* **52**, 89 (2016).
 [7] N. Sokołowska, PhD dissertation, University of Warsaw, in preparation.

Reaction with ^9Li at HIE-ISOLDE

Result of experiments IS561

Jesper H. Jensen for the IS561 collaboration

The final part of the IS561 experimental campaign was carried out in the beginning of November 2018. The three experiments included in this campaign set out to investigate the nuclear structure of ^{11}Li as well as the two subsystems ^{10}Li and ^9Li . The goal is to populate single particle states by neutron transfer to ^9Li . This is possible at ISOLDE due to the availability of a high purity and high yield ^9Li beam.

For the $d(^9\text{Li},p)^{10}\text{Li}$ reaction we used a ^2H (deuterated polyethylene) target and for $t(^9\text{Li},p)^{11}\text{Li}$ we used a ^3H target on a Ti backing. The ^2H target was used both at 6.7 MeV/A and 8 MeV/A, whereas the ^3H target was used only at 8 MeV/A.

Due to the relatively large kinematic compression that comes along with inverse kinematics, we need to enter the regime of 6-10 MeV/A to measure in the backward laboratory directions. This has become possible with the recent successful developments of HIE-ISOLDE.

Beside the HIE-ISOLDE upgrades, the experimental setup at the Scattering Experiment Chamber (SEC) has been improved in terms of both electronics, detector setups and data acquisition. One example is the implementation of the *shadowed readout-mode*[1], which allows us to take much larger data rates before we are limited by significant deadtime.

Results

In the last IS561 experiment, we ran with the ^3H target as well as a Ti-target for background measurements. The background from Ti turned out to be essentially negligible. This was a major concern prior to the ex-

periment since we are well above the Coulomb barrier. With such a small background from Ti, the conditions for this experiment were excellent.

Unfortunately, we experienced issues with the ^3H target. We saw a large unexpected background of protons, the particle of interest in the two-neutron transfer reaction $t(^9\text{Li},p)^{11}\text{Li}$, see Figure 1. We believe that it came from a glue-like component, that was applied during a recent remount of the target foil to the target holder as well as a steel-like component from the target holder itself.

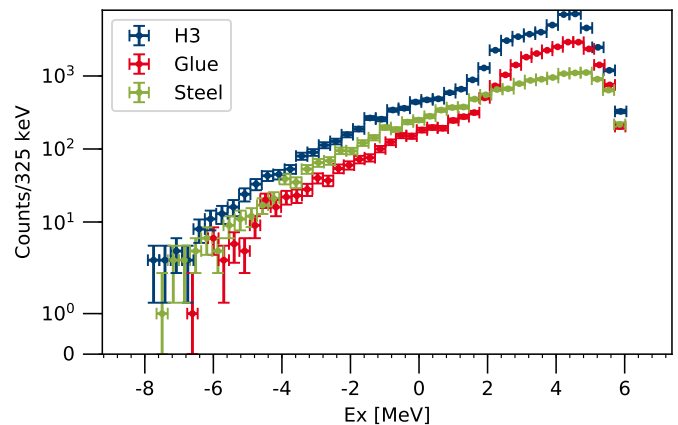


Figure 1: ^{11}Li excitations spectra for identified protons. The three curves corresponds to three different regions on the target. Unfortunately the glue and steel parts seems to reconstruct the nominal (^3H) signal.

This means that the present data give a very limited possibility to extract the type of physics we expected. The analysis is, however, ongoing in an effort to extract possible limits on the cross sections in different angular ranges.

Besides the primary ^3H target, we also ran with a ^2H target. These measurements were succesful. We clearly identify both p, d and t. These measurements

were performed both at 6.7 MeV/A and 8 MeV/A. The analysis is ongoing, as well as theoretical calculations performed by A. Moro *et al.* The results from these will complement the data from the IS367 campaign, where ${}^9\text{Li}$ impinging on a deuterated target were performed with beam energies 2.4 MeV/A and 2.8 MeV/A.

References

- [1] M. Munch, J. H. Jensen, B. Loher, H. Tornqvist, H. T. Johansson, *IEEE Transactions on Nuclear Science* **66**(2), 575 (2019).

Other News

MEDICIS Operation in 2018 and plans for LS2

*Joao Pedro Ramos, Thierry Stora
for the MEDICIS Coordination and Collaboration*

The MEDICIS facility aims at becoming a leading European facility for the production of non-conventional medical isotopes for research in treatment and diagnosis, notably exploiting electromagnetic mass separation. The MEDICIS Collaboration Memorandum of Understanding (MoU) was signed in 2018 by CERN, KU Leuven (BE), the Accelerator for Research in Radiochemistry and Oncology at Nantes Atlantic (FR), the National Physical Laboratory (UK), Instituto Superior Técnico (PT), Centre Hospitalier Universitaire Vaudois (CH), Hôpitaux Universitaires de Genève (CH), Institut Laue-Langevin (FR/EU) and Fundació Andaluza Beteria para la Investigació en Salut (ES). In addition, several partners which are already collaborating with MEDICIS are making the final adjustments to officially join the collaboration: Paul Scherrer Institute (CH), Riga Stradins University (Latvia), the JRC-Directorate G (EU).

First operation with radioactive beam started in May 2018, after a short commissioning phase in December 2017. During 2018, more than 20 irradiations took place with more than 10 targets for machine development (MD) and experiments (MEDxxx), as approved by the MEDICIS board. Steady progress was achieved while reaching the proposed milestones: a terbium release efficiency of - 5 % with rhenium surface ion source, 100MBq range activities, and operation with Uranium Carbide targets. Current isotopes produced at MEDICIS include: ^{149}Tb , ^{152}Tb , ^{155}Tb , ^{169}Er and ^{165}Tm . Developments are being made to extend this list to ^{47}Sc , ^{44}Sc , ^{67}Cu and $^{225}\text{Ra/Ac}$. Furthermore, at the end of 2018, two irradiations scheduled at the MEDI-

CIS point (6 days) allowed for a total of 18 days of extra beam time (winter physics programme) for IS554 (^7Be) and IS657 ($^{223,225,226}\text{RaF}$), showing the good synergy with ISOLDE.



Figure 1: Road transportation with type A container containing ^{149}Tb MEDICIS collection for delivery to CHUV; figure inset - salt coated aluminum foil.

While CERN has currently entered its accelerator shutdown (LS2 - 2019/2020), MEDICIS will be able to resume operation in April 2019. Instead of producing the isotopes with 1.4 GeV PSB beam they will be provided as non-separated external sources from partners cyclotrons and nuclear reactors (e.g. Er, Tb, Sc, Ra/Ac). From January to March 2019, the technical stop at MEDICIS will allow for maintenance and upgrade: (i) replacement of the extraction electrode movement mechanism, (ii) addition of a magnet shunt to improve beam profile, (iii) installation of a 5cm lead thick fume hood for radiochemistry, (iv) finalization of MELISSA (MEDICIS Laser Ion Source Setup at CERN), (v) ventilation, cooling, gas, high/low voltage and robot maintenance and (vi) obtainment of a new facility permit which will allow operation with lasers, radiochemistry and higher activities. At the end of March MEDICIS will enter into commissioning and will finally

be back into operation.

A new collection foil has been tested this year to facilitate the subsequent radiochemistry process. The usual 500 nm zinc coated gold foil was replaced with a KNO_3 salt layer (see figure 1) on an aluminum foil, which is simply dissolved by water instead of strong acid. This was used to ship a ^{149}Tb sample collected in the oxide sideband to CHUV. On the MELISSA side, the final installation is being completed and after commissioning, improvement factors of more than 10 in efficiency are expected for Tb and Er.

In the planning for 2019 [1] MEDICIS intends to extract ^{155}Tb (from ARRONAX) and ^{169}Er (from ILL) with MELISSA and radiochemistry purification, and develop the separation of actinium/radium and of $^{44/47}\text{Sc}$ as ScF_x molecules.

References

- [1] 'MEDICIS 2019 Tentative schedule, v1 (February 2019)', CERN Accelerator Schedule Management.

ISOLDE support

Access and contacts

1. Use the online pre-registration tool¹ which should be launched by your team leader or deputy team leader. You need to attach the following documents to the pre-registration:
 - **Home Institution Declaration² signed by your institute's administration (HR).**
 - Passport
2. When your pre-registration is accepted by the CERN users office you will receive an email telling you how to activate your CERN computer account. However, you cannot activate your CERN EDH account until you arrive at CERN and complete the registration process.
3. When you arrive at CERN go to the Users office to complete your registration (Opening hours: 08:30 - 12:30 and 14:00 – 16:00 but closed Wednesday mornings).
4. Get your CERN access card in **Building 55**
5. Follow the online mandatory CERN safety courses: safety at CERN; Radioprotection awareness and emergency evacuation.
 - If you have activated your CERN account, you can access the mandatory courses online at the web page lms.cern.ch, from your computer, inside or outside CERN.
 - If you have not activated your CERN account, there are some computers available for use without the need to log in on the first floor of building 55 (Your CERN badge will be needed in order to prove your identity).
6. Complete the following online courses available at <https://lms.cern.ch>:
 - **ISOLDE RP course for Supervised Radiation Areas "Radiation Protection - Supervised Area".**
 - **Electrical Safety - Awareness Course - Fundamentals**
 - **Electrical Safety - Awareness Course - Facilities**

If you have not activated your CERN account see the second part of entry 5.
7. Obtain a Permanent radiation dosimeter at the Dosimetry service, located in Building 55³ (Opening hours: Mon. to Fri. 08:30 – 12:00). *If you do not need the dosimeter in the following month it should be returned to the Dosimetry service at the end of your visit.* The "certificate attesting the suitability to work in CERN's radiation areas"⁴ signed by your institute will be required.
8. Follow the practical RP safety course and Electrical Awareness Module for which you will have to

¹For information see [the CERN users' office](#)

²The Home Institute Declaration should not be signed by the person nominated as your team leader.

³<http://cern.ch/service-rp-dosimetry> (open only in the mornings 08:30 - 12:00).

⁴The certificate can be found via <http://isolde.web.cern.ch/get-access-isolde-facility>

⁵For information about how to register see <http://isolde.web.cern.ch/get-access-isolde-facility>

register in advance⁵. These take place on Tuesday afternoons from 13:00 until 17:00 at the training centre (building 6959) in Preveessin. If you do not have your own transport, you can take CERN shuttle 2 from building 500. The timetable for this is [here](#).

9. Apply for access to "ISOHALL" using ADAMS: <https://www.cern.ch/adams>. (This can be done by any member of your collaboration (typically the contact person) having an EDH account⁶). Access to the hall is from the Jura side via your dosimeter. Find more details about CERN User registration see the [Users Office website](#). For the latest updates on how to access the ISOLDE Hall see the [ISOLDE website](#).

New users are also requested to visit the ISOLDE User Support office while at CERN. Opening hours: Monday to Friday 08:30 - 12:30

Contacts

ISOLDE User Support

Jenny Weterings
Jennifer.Weterings@cern.ch
+41 22 767 5828

Chair of the ISCC

Bertram Blank
blank@cenbg.in2p3.fr
+33 5 57 12 08 51

Chair of the INTC

Karsten Riisager
kvr@phys.au.dk
+45 87 15 56 24

ISOLDE Physics Section Leader

Gerda Neyens
gerda.neyens@cern.ch
+41 22 767 5825

ISOLDE Physics Coordinator

Karl Johnston
Karl.Johnston@cern.ch
+41 22 767 3809

ISOLDE Technical Coordinator

Richard Catherall
richard.catherall@cern.ch
+41 22 767 1741

ISOLDE Deputy Technical Coordinator (with special responsibility for HIE-ISOLDE)

Erwin Siesling
erwin.siesling@cern.ch
+41 22 767 0926

More contact information at

[ISOLDE contacts](#) and at [ISOLDE people](#).

⁶Eventually you can contact Jenny or the Physics coordinator.